AD-A120 575 ANALYSIS OF TRAVELING WAVE TUBE MATERIALS(U) AIR FORCE 1/1
WRIGHT AERONAUTICAL LABS WRIGHT-PATTERSON AFB OH
B C LAMARTINE ET AL. MAR 82 AFWAL-TR-81-4115

UNCLASSIFIED F/G 9/1 NL

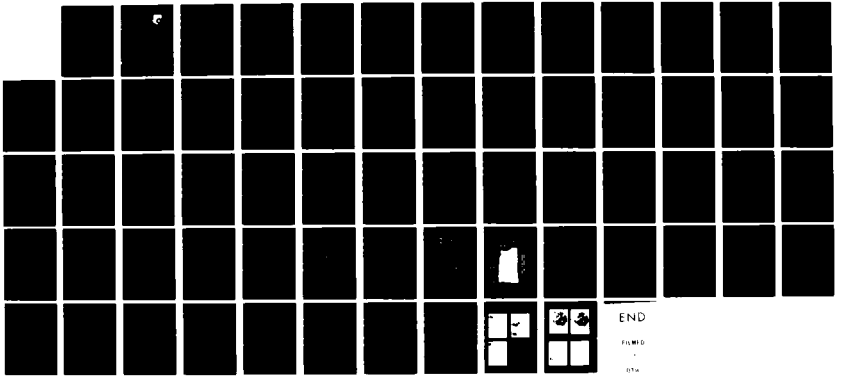

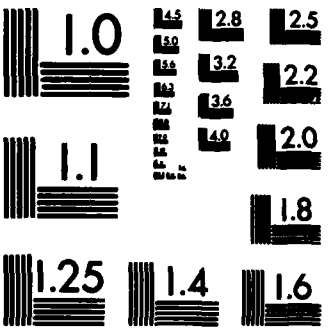

(12)

AFWAL-TR-81-4115

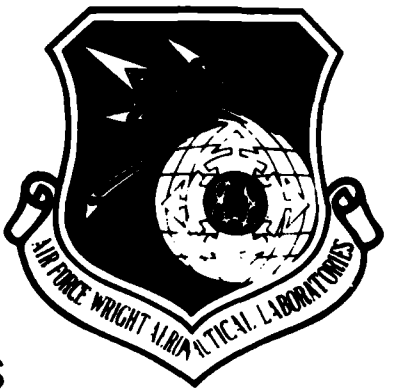

ANALYSIS OF TRAVELING WAVE TUBE MATERIALS

B. C. Lamartine
W. V. Lampert
K. D. Rachocki
W. L. Baun
T. W. Haas
Mechanics and Surface Interactions Branch
Nonmetallic Materials Division

March 1982

Final report for period October 1977 - October 1980.

Approved for public release; distribution unlimited.

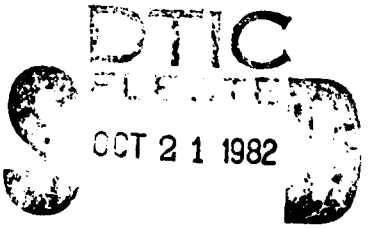

A

MATERIALS LABORATORY
AIR FORCE WRIGHT AERONAUTICAL LABORATORIES
AIR FORCE SYSTEMS COMMAND
WRIGHT-PATTERSON AIR FORCE BASE, OHIO 45433

NOTICE

When Government drawings, specifications, or other data are used for any purpose other than in connection with a definitely related Government procurement operation, the United States Government thereby incurs no responsibility nor any obligation whatsoever; and the fact that the government may have formulated, furnished, or in any way supplied the said drawings, specifications, or other data, is not to be regarded by implication or otherwise as in any manner licensing the holder or any other person or corporation, or conveying any rights or permission to manufacture, use, or sell any patented invention that may in any way be related thereto.

This technical report has been reviewed and is approved for publication.

BRUCE C. LAMARTINE, Project Engineer
Mechanics & Surface Interactions Branch
Nonmetallic Materials Division

S. W. TSAI, Chief
Mechanics & Surface Interactions Branch
Nonmetallic Materials Division

FOR THE COMMANDER:

FRANKLIN D. CHERRY, Chief
Nonmetallic Materials Division

"If your address has changed, if you wish to be removed from our mailing list, or if the addressee is no longer employed by your organization please notify AFWAL/MLBM *,W-P AFB, OH 45433 to help us maintain a current mailing list".*

Copies of this report should not be returned unless return is required by security considerations, contractual obligations, or notice on a specific document.

Unclassified

SECURITY CLASSIFICATION OF THIS PAGE (When Data Entered)

REPORT DOCUMENTATION PAGE

READ INSTRUCTIONS BEFORE COMPLETING FORM

1. REPORT NUMBER: AFWAL-TR-81-4115	2. GOVT ACCESSION NO.
3. RECIPIENT'S CATALOG NUMBER	
4. TITLE (and Subtitle): ANALYSIS OF TRAVELING WAVE TUBE MATERIALS	5. TYPE OF REPORT & PERIOD COVERED: Internal, October 1977 to October 1980
	6. PERFORMING ORG. REPORT NUMBER
7. AUTHOR(s): B. C. Lamartine, W. V. Lampert, K. D. Rachocki, W. L. Baun and T. W. Haas	8. CONTRACT OR GRANT NUMBER(s): In-House Report
9. PERFORMING ORGANIZATION NAME AND ADDRESS: Materials Laboratory (AFWAL/MLBM), Air Force Wright Aeronautical Laboratories, Wright-Patterson AFB OH 45433	10. PROGRAM ELEMENT, PROJECT, TASK AREA & WORK UNIT NUMBERS: Project 2303, Task 2303Q104 WUD# 41
11. CONTROLLING OFFICE NAME AND ADDRESS: Materials Laboratory (AFWAL/MLB), Air Force Wright Aeronautical Laboratories, Wright-Patterson AFB OH 45433	12. REPORT DATE: March 1982
	13. NUMBER OF PAGES: 64
14. MONITORING AGENCY NAME & ADDRESS (if different from Controlling Office)	15. SECURITY CLASS. (of this report): UNCLASSIFIED
	15a. DECLASSIFICATION/DOWNGRADING SCHEDULE

16. DISTRIBUTION STATEMENT (of this Report)

Approved for public release; distribution unlimited.

17. DISTRIBUTION STATEMENT (of the abstract entered in Block 20, if different from Report)

18. SUPPLEMENTARY NOTES

19. KEY WORDS (Continue on reverse side if necessary and identify by block number)

Traveling Wave Tubes (TWT)	AES
Cathodes	XPS
Getters	ISS
	SIMS

20. ABSTRACT (Continue on reverse side if necessary and identify by block number)

A wide variety of materials are utilized in the construction of traveling wave tubes (TWT) used as microwave amplification elements for many Air Force applications. The only active component is the cathode which is heated to thermionic temperatures to serve as the electron emitting element in the electron gun section of the tube. Considerable interest exists in the correct scientific model of an activated cathode. Most such cathodes are barium-based and this research program has shown that barium in the metallic state is necessary on the surface of dispenser cathodes in order to get an acceptably

DD FORM 1 JAN 73 1473 EDITION OF 1 NOV 65 IS OBSOLETE

Unclassified

SECURITY CLASSIFICATION OF THIS PAGE (When Data Entered)

low (~2.1eV) work function. Other TWT materials investigated in this program include an evaluation of the electron bombardment resistance of boron nitride insulators and the determination of the activation mechanism and characteristics of nonevaporable zirconium-graphite getters. Other failure analysis investigations of TWT's are also reported herein.

FOREWORD

This is the final report for work unit 2303Q104, "Analysis of Traveling Wave Tube Materials". The work reported here was carried out during the period October 1977 to October 1980 as an in-house basic research program in the Nonmetallic Materials Division of the Air Force Wright Aeronautical Laboratories/Materials Laboratory at Wright-Patterson Air Force Base. The work unit leader was Capt Bruce Lamartine.

Thanks are due to many people for their contributions to this program but a special mention should be made of the many technical suggestions and contributions of Dr. F. M. Wachi of the Aerospace Corporation. The assistance of the SD/YKD and YKX program offices is also gratefully acknowledged.

TABLE OF CONTENTS

LIST OF TABLES

LIST OF ILLUSTRATIONS

LIST OF ILLUSTRATIONS (Continued)

SECTION I

INTRODUCTION

Traveling wave tubes (TWT's) are important microwave amplification devices used in a wide variety of Air Force applications including radar and electronic countermeasure (ECM) power amplification components and as satellite communication elements. In radar and ECM applications the emphasis in TWT design is on power, efficiency, size, weight and cost; while in satellite applications the emphasis is on reliability and long life. At this time no adequate solid-state microwave amplifier is available to cover the power-frequency domain required both for current and future applications. It thus is quite important to improve the reliability, manufacturing yield, lifetimes and to reduce costs of these TWT's. Many of those goals can be achieved by improved manufacturing technology, through tube redesign and by changes in procurement philosophy. However, it is also apparent that TWT's, while deceptively simple in appearance, are a veritable laboratory in materials technology. Many opportunities for development of improved materials and processes exist and many investigations of the interactions of materials with the tube environments (vacuum, high temperatures, electron and ion bombardment, etc.) both inside the tube and out need to be made. The goal of this research program has been to apply modern surface analysis methods, such as Auger electron spectroscopy (AES), x-ray photoelectron spectroscopy (XPS or ESCA), secondary ion mass spectrometry (SIMS), and ion scattering spectroscopy (ISS) to a variety of surface science related material problems in TWT applications. This is the final report for in-house work unit 2303Q104, Analysis of Traveling Wave

Tube Materials, which is terminated via this report, and will summarize research results on barium-based dispenser cathodes, electron bombardment resistance of helix support rods such as BN and BeO, and characteristics of nonevaporable zirconium-graphite getters. In addition, the results of some failure analysis activities on Defense Satellite Communications System (DSCS) satellite TWT's will be recorded.

SECTION II

EXPERIMENTAL TECHNIQUES EMPLOYED

The surface analysis techniques employed in this program include scanning Auger microscopy (SAM), XPS or ESCA, ISS and SIMS. The instruments employed were commercially available ones and included a Physical Electronics Industries Model 550 SAM/ESCA system, a Minnesota Mining and Manufacturing 3M Model 525 Ion Scattering Spectrometer and a Physical Electronics Industries Model 548 SAM system. Standard instrumental techniques were, for the most part, employed. Several good summaries of each of these are available (References 1 and 2) and no detailed discussion of each technique will be given here.

Instrumental parameters employed for SAM measurements were typically an incident beam of 4KeV energy and 1 μamp current into a 5-10 micron diameter spot size. Detection was done by phase sensitive modulation methods using typically 1-6eV P-P sine or square wave modulation. XPS measurements were made with a nonmonochromatized Mg K_α soft x-ray source. Typical pass energies on the spectrometer were 100eV for wide energy survey scans and 25eV for narrow, high resolution scans. Photoelectron peaks were measured with the Mg K_α x-rays taken as 1253.6eV and with the Au 4§ photoelectron line referenced to 83.8eV. ISS measurements were made using He+ ion beams of energy 0.3 to 2KeV. Typical currents were 1 μamp. A UTI quadrupole gas analyzer with a single ion energy filter attached was used to make simultaneous SIMS measurements.

Work function measurements on cathodes were made using a close-spaced diode configuration. Both water cooled anodes and thin Mo foil

anodes which were flashed to high temperatures to obtain a near atomically clean surface were employed. Simple effective work function measurements as described by Hensley (Reference 3) were frequently used although some dip test measurements were also made and analyzed according to the work of Maurer (Reference 4) and Dominguez, Doolittle and Varadi (Reference 5). A computer program written for a hand calculator provided a convenient way to analyze this data.

Ba evaporation sources were obtained from SAES Getters, Inc. They consisted of a resistantly heated channel containing a Ba alloy. Purities of evaporated films were checked in several ways, the most sensitive being a SIMS measurement which showed very minor amounts of oxides, nitrides and hydrides, and no metallic impurities except a small trace (300 PPM) of aluminum.

SECTION III

SURFACE CHARACTERIZATION OF IMPREGNATED TUNGSTEN DISPENSER CATHODES

1. INTRODUCTION AND BACKGROUND

There are primarily two models for cathode activation that have gained acceptance in the scientific literature. No attempt will be made to evaluate all previous research done or to prove the validity of one model vs. the other as this has been done in several very good review articles (References 6, 7, and 8). The two models in question are the defect semiconductor model and the thin film dipole model. They can be described briefly as follows: The defect semiconductor model is predicted on the existance of a layer of barium oxide in the surface regions of the cathode. As the cathode temperature is raised during activation some of the BaO either reacts chemically with substrate materials or with activators in the substrate and/or some homogeneous decomposition of the BaO occurs. The oxygen is then either desorbed as atomic oxygen or diffuses into the substrate and is bound there. The net result is a nonstoichiometry BaO layer with oxygen deficiencies. The effects of this nonstoichometry can be understood in terms of the energy levels in the semiconductive BaO by referring to Figure 1. As pointed out by Haas, Shih and Thomas, the work function, ϕ, is the sum of the electron affinity, χ, and the position of the conduction band edge, E_c, relative to the fermi level:

$$\phi = \chi + E_c \qquad (1)$$

A lowering of the work function can occur if either χ or E_c are decreased. Haas et. al., (Reference 9) have made measurements on single crystal BaO films on single crystal Ir substrates using a low energy electron reflection (LEER)

technique and through a simple kinematical analysis of these data claimed to be able to separate out the two components. Their results indicated that the χ value was most dependent on surface dipole changes whilst the E_c value was dependent on bulk chemical and physical states. Low work function values of these thin film single crystal sandwiches were obtained by "activating" the sandwich through thermal treatment, the effect being a decrease in E_c with χ remaining virtually unchanged. Whether such results can be extrapolated to actual cathode phenomena, particularly impregnated tungsten dispenser cathodes, remains unproven.

The second cathode model, the thin film dipole model, postulates the existence of a thin layer of material, e.g., Ba in the metallic state, on the surface. This layer, perhaps only one monatomic layer thick, causes a surface dipole to be created which results in a lowered potential barrier to electron emission.

The correctness of the model used to describe cathode activation and operating mechanism is of more importance than scientific curiosity. When considering life limiting factors one approaches the situation differently for the two models. If, for example, the semiconductor model is appropriate then the cathode will be extremely sensitive to trace element poisoning as it is well known that allowed semiconductor energy levels and electronic states are very sensitive to dopants. Further, the defect state produced during activation may be easily poisoned by active residual gases such as oxygen and not easily regenerated. Finally, sputtering of the activated layer will be very deleterious to long term operation. In the thin film model, on the other hand, a chemical reaction is postulated that regenerates the thin film active layer. Of importance to lifetime in this case are the chemical reactions to produce the active Ba layer, the transport of the

Ba to the surface region, its evaporation rate from the surface, and the amount of surface coverage needed to produce the required work function lowering.

Although the two proposed models are distinct in concept, in fact, when carried far enough they have some similarities. A very oxygen deficient BaO film is not greatly different than postulating a Ba metallic film on a BaO thin film substrate. It is further not unexpected that elements of both models may be required to obtain the very best cathode performance as may be required in long lived spaceborne TWT's. This may be particularly the case for oxide cathodes where the chemistry and physics of activation and operation seem to be the most complex. In recent work Haas, Shih and Thomas (Reference 10) performed surface analysis and work function measurements on a series of oxide cathodes and concluded that the semiconductor model could explain their observed results. On the other hand the work functions measured by them for oxide cathodes on nickel substrate without activators present were higher than would be acceptable to a production tube engineer. The addition of an activator may in fact result in the generation and adsorption of Ba metal onto a defect BaO/SrO crystallite thus providing two mechanisms for optimum activation.

2. EXPERIMENTAL PROCEDURE AND RESULTS

The work to be described in this section will cover only impregnated tungsten dispenser cathodes and not oxide type cathodes. Utilization of modern surface analysis techniques would appear to offer great hope in determining the presence or absence of thin films of metallic Ba on W substrate such as would be obtained if a thin film model applies for a dispenser cathode. The use of x-ray photoelectron spectroscopy would seem

to be most appropriate as it is well known that binding energy shifts of core electrons in atoms going from the metallic to the oxide state undergo shifts of several eV, which the XPS technique can easily measure. To utilize XPS measurements, however, required previous measurements of known compounds and thin film structures in order to properly identify cathode surface chemistry changes. A search of the scientific literature did not yield any adequate previous XPS measurements of Ba and its compounds. The first stages of this work required measurements of standard Ba compounds. The results obtained are contained in several journal articles (References 11 and 12) and may be summarized as follows: the two most promising photoelectron groups to monitor are the $3d_{3/2}$, $3d_{5/2}$ lines and the $4d_{3/2}$, $_{5/2}$ lines. Concurrently one also obtains photon excited Auger spectra and here the most intense group to follow is the MNN transition series. Fortunately, none of these transitions overlap other important lines, such as those from W, O, C, N, Ca, or Al, that might be expected on the dispenser cathode surface. A summary of the measurements of these lines, using the Au $4f_{7/2}$ line with a binding energy of 83.8eV as reference point, is given in Table 1. The thin film structures were obtained as described by Moore and Allison (Reference 13) and by Forman (Reference 14) and are produced as described schematically by Figure 2. The basis of these structures is the observation that heating clean W covered by thick Ba films to 1000°K for one minute in ultra-high vacuum causes all but the last monolayer to evaporate. These structures are most appropriate to the interpretation of cathode measurements as we shall see later. The data in Table 1 show two important facts about the surface chemistry of Ba. First, only minor shifts in energy are observed in going from the metallic to the oxide state (<1eV); and second, the shift is opposite to that which normally occurs in XPS measurements (Reference 1). This latter observation can be explained in terms of

relaxation effects and has been observed with Ag and Cd as well (References 15 and 16). The small shifts observed severely limit the utility of direct binding energy shift measurements in discerning Ba chemical states. An alternative to this measurement, which is considerably more distinctive, is the use of energy difference measurements. Experience on model compounds shows that a measurement of the binding energy separation between the $3d_{5/2}$ photoelectron and the $M_4\ N_{4,5}N_{4,5}$ Auger transition is a reliable and easily measured quantity which can be used to determine chemical states of Ba. These Auger-Photoelectron Energy Separations (APES) are tabulated in Table 1 for reference. The APES method has the additional benefit that sample charging and biasing will not affect the quantity, as both Auger and Photoelectrons would shift the same amount due to those perturbations. A typical XPS spectrum illustrating the APES measurement is shown in Figure 3. Plots of the APES can be made as shown in Figure 4. Since the Auger and photoelectron energy axes are on the same scale, a 45° straight line can be plotted through the points for the various structures. Sample charging and/or biasing will then simply shift the coordinates for a measurement of any given chemical state along one of these straight lines, while changes in chemical state will move the coordinate from one line to another.

Changes in the Ba surface chemistry of an impregnated tungsten dispenser cathode during initial activation in ultra-high vacuum can be plotted on the APES plots and one such example is shown in Figure 4. Initially, as expected, the points fall on the oxide line. As the temperature in raised, however, the APES points move away from the BaO line towards the Ba metal line. At the point of activation and electron emission, however, no further points can be plotted due to a severe change in shape of the Auger feature. This is illustrated in Figure 5; a flat region now exists where before a peak

was observed. Subsequent analysis of this feature showed that it can be generated by adding together the Auger features of Ba metal and the Ba-O-W thin film sandwich. More recent analysis by Springer and Lamartine (Reference 17) of the 3d photoelectron lines shows that they can indeed be deconvoluted into two components separated by roughly 0.8eV in energy. These facts lead to a conclusion that Ba in the metallic form is required for dispenser cathode activation and because the Ba layers found on activated cathodes are no more than 2 atomic layers thick would tend to support the thin film model for this type of cathode.

A next question of importance is the configuration of the Ba films formed during activation, i.e., is the Ba on top, or is a mixed surface layer present, or is the oxygen on top. The ISS technique is ideally suited to such determinations. Under conditions of low energy elastic ion scattering, the probability of binary collisions without ion neutralization is sufficiently low that virtually all scattering information is limited to the top atomic layer of the solid. Results of the ISS measurement taken from activated cathodes at operating temperatures utilizing low energy (300eV) Ne^+ ions are shown in Figure 6. This figure shows the surface to be a predominantly Ba layer. In fact, the small amount of W shown in the spectrum is due to the removal of the outer Ba layer by a sputtering mechanism during the time the measurements took place (Reference 18). Subsequent measurements with continuous bombardment does remove the Ba layer which appears to be very loosely bound and easily sputtered away.

3. CONCLUSIONS, OTHER OBSERVATIONS AND FUTURE WORK

The results of the measurements made to date on impregnated tungsten dispenser cathodes lead to a model proposed by Forman (Reference 14) and illustrated in Figure 7. The impregnant in the pores of the tungsten plug reacts chemically according to some reactions such as

$$W + 6BaO \rightarrow Ba_3WO_6 + 3Ba$$

$$\text{and } W + 2Ba_3WO_6 \rightarrow 3BaWO_4 + 3Ba$$

The Ba metal generated in the pores then migrates by some sort of diffusion mechanism, likely interfacial, to the surface of the cathode where monolayers or partial monolayers form on the surface. Evaporation of the Ba at operating temperatures will then be an important life limiting mechanism. As a result, during life more and more of the BaO and W in the bulk of the cathode disc will be consumed and eventually an insufficient amount will remain to keep the surface Ba at a high enough level for proper tube operation.

Considerable work on dispenser cathode phenomena remains to be done before reliability and predictability of the kind required in long life space tube applications is acheived. The more important tasks remaining are 1) a determination of the quantity of Ba metal on the surface vs. the work function; 2) the effects of varying the impregnant mixture composition (ratio of BaO: $CaO:Al_2O_3$); 3) the effects of porosity and pore size distribution in the W plug; 4) the determination of evaporation rate as a function of these several variables, and finally 5) the role of poisoning elements such as Fe, S, etc., in raising the work function of a dispenser cathode.

SECTION IV

EVALUATION OF ELECTRON BOMBARDMENT RESISTANCE OF ANISOTROPIC AND ISOTROPIC BORON NITRIDE

1. INTRODUCTION AND BACKGROUND

The use of various ceramic insulators in TWT's as supports for helixes, cathodes, gun elements and the like always raises the question of the possibility of electron beam degradation of the material. In general this degradation may proceed by decomposing the materials, for example the reduction of silicon dioxide to elemental silicon with the evolution of gaseous oxygen, or by the mechanism of electron beam evaporation. Many examples of both types of behavior are known and are well documented in the scientific literature. A question of some current concern is whether or not boron nitride might undergo a degradation mechanism such as:

$$2BN \xrightarrow[\text{bombard}]{\text{electron}} 2B + N_2$$

when used as a helix support material in TWT's. Obviously if this mechanism occurs to any degree during the lifetime of the tube two deleterious results will follow: first, the nitrogen will raise the pressure in the tube above acceptable limits and may cause severe ionic bombardment and destruction of the cathode. Second, the boron metal produced, being nonvolatile, may form a conductive coating on the rod, leading to excessive helix currents. The investigation of this possible process is the basis for this report.

Boron nitride itself is available in two crystalline forms, isotropic and anisotropic. A seondary question, then to be answered, is whether significant differences exist in the probability for e-beam degradation of either form.

Finally, some data of the charging behavior of BN was also obtained both for normal and nonnormal indicent electron beams.

2. EXPERIMENTAL PROCEDURES

A variety of experiments were performed with techniques to look at changes in surface composition, surface chemistry and products evolved from the BN during e-bombardment. The electron bombardments were generally performed with 3 to 5 KeV beams using from 5 to 50 μA current using either a grazing incidence electron gun or the electron gun in the Auger spectrometer.

The experiments conducted were:

a) Measurement of the ratio of the B to N peak heights in an Auger spectrometer over a long period of time on a BN sample undergoing intense electron bombardment. Changes in the B to N ratio would be indicative of e-beam decomposition. A sample of such an experiment is shown in Figure 8.

b) Measurements of peak shape changes in Auger spectra of B and N following long time electron beam exposure. It is well known that the shapes of Auger features for many elements are a good fingerprint for the chemical form of that element (Reference 19). Samples of the results obtained are shown in Figure 9.

c) Attempts were made to detect any ionic fragments emitted by BN during electron bombardment. This was accomplished by signal averaging the output of a secondary ion mass spectrometer system while the BN sample was given a heavy electron bombardment. This experiment gave no measurable signal.

d) The ESCA spectra of several BN samples were taken before and after heavy electron bombardment doses. The photoelectron energies shift by easily measurable amounts when going from pure elements to their oxides or other chemical form. Thus the presence of two sets of lines for B, for example,

would indicate two chemical forms, one perhaps nitride and the other perhaps metallic B. ESCA spectra of pure BN before bombardment and afterwards are shown in Figure 10.

e) It is possible that BN is desorbed by the electron beam as neutrally charged molecular species. This possibility was tested in a flag experiment in which a cleaned metal foil was placed in a position next to a sample of BN that was being heavily electron bombarded such that any desorbed species would have a high probability of condensing on the metal foil. The metal was then subsequently rotated to a position where Auger electron spectroscopic analyses could be performed. No B or N ascribable to this mechanism was detected.

f) The final set of experiments involved measuring the SIMS from BN both before and during electron bombardment while looking for changes in the B to N ratio or for other changes in the SIMS fingerprint. A typical SIMS spectrum is shown in Figure 11.

3. RESULTS

The results obtained in all the above experiments can be briefly summarized by stating that all produced a negative result. It is, perhaps, useful to try to make some approximate upper bound for the bombardment induced decomposition cross section using the best approximations from known experimental parameters. Bear in mind that these are, in fact, estimates and can be in error by significant amounts.

The calculation of the cross section will be made with these assumptions:

a) The density of atoms in the BN is 10^{15} atoms/cm^2

b) A change in chemical state of composition of 10% would be detectable. Thus, damage to 10^{14} atoms/cm^2 or more would be detectable by the various

experiments. This is clearly an underestimate but allow for some other possible overestimates.

c) The current density of the bombarding electrons (assumed to be uniform in cross-section) is 50 μA focused into a 0.4 mm diameter spot.

Using these assumptions and with an average bombardment time of 12 hours (also an underestimate by about a factor of 2-5) and if we define a cross section for damage, σ, as

$$\sigma = \frac{\text{surface atoms damaged}}{\text{incident electron}}$$

then

$$\sigma \leq \frac{10^{14}\ \text{atom/cm}^2}{\frac{50 \times 10^{-6}\text{A}}{(.02)^2\text{cm}^2}\ \frac{\text{coulomb}}{\text{A - Sec}} \times (12 \times 60 \times 60)\ \text{Sec} \times \frac{\text{electrons}}{1.6 \times 10^{-19}\ \text{coulomb}}}$$

$$\leq .93 \times 10^{-8}\ \frac{\text{atoms}}{\text{electron}} \quad \text{or} \quad \frac{10^{-8}\ \text{atoms damaged}}{\text{incident electron}}$$

To see the effects of such a damage rate consider the case where 1 cm^2 of BN is exposed to a current density of 100μA/cm^2 for a time of 1 hour. The total number of nitrogen atoms released (presumming all surface electron bombardment damage results in one nitrogen desorbed, again an overestimate of the damage) would be:

$$n_N(\text{gas}) = \frac{10^{-8}\ \text{atoms}}{\text{electron}} \times 100\mu\text{A} \times 3600\ \text{Sec} \times \frac{10^{-6}\ \text{amp}}{\text{A}} \times \frac{\text{electron}}{1.6 \times 10^{-19}\ \text{coulomb}}$$

$$= 2 \times 10^{+10}\ \text{atoms desorbed.}$$

The impact of this worst case situation can be seen in terms of the pressure rise inside the TWT. Considering the volumne of the tube

to be 5 cm^3 this rise would be equivalent to a partial pressure of N atoms (not realistic as they would undoubtedly combine to form N_2) of:

$$p = \frac{nRT}{V} = \frac{2 \times 10^{10} \text{ (atoms N)} \times 298^\circ \text{ K}}{5 \text{ cm}^3} \times \frac{10^{-19} \text{ torr cm}^3}{\text{atom } ^\circ\text{K}}$$

$$= 1.2 \times 10^{-7} \text{ torr}$$

Considering the fact that the tube itself acts as a pump, it is not likely that such pressure rises would ever occur. Further, more realistic estimates of cross sections, etc., probably reduce this figure by one to three orders of magnitude.

4. CONCLUSIONS, OTHER OBSERVATIONS, AND FUTURE WORK

It is difficult to calculate the total amount of electron bombardment which insulators in a functioning tube may receive. The temperature at which the insulator is held may also be an important parameter. Our equipment is not configured in such a way as to allow bombardment of BN while hot. Future improvement will, however, provide this capability and perhaps these experiments should be performed. Nonetheless the totally negative results relative to any indication of BN degradation should provide some degree of confidence in its use. It should be added that these results were identically negative for both the isotropic and anisotropic forms of BN.

During the course of electron bombardment it was observed that an increase in carbon, accompanied by a darkening in the bombarded region, had occurred. The pressure in the system during the experiment was in the 10^{-11} torr range in many of the measurements taken which should compare favorably with conditions inside sealed tubes. Hence the possibility is strong that similar cracking of hydrocarbons on surfaces inside tubes is occurring. This may, in fact, be beneficial if not carried too far. The

carbon layer, while too thin to be electrically conductive, could absorb most of the damage from the electron beam, hence, improving bombardment resistance. Its effects on dielectric losses from the RF wave, however, may be deleterious (Reference 29). A study of the surfaces of components from failed nearly good vs. very bad tubes might be of value here.

The Auger and ESCA analyses of BN always showed a measurable amount of oxygen present in the BN. It does not appear to be simply a surface layer but persists through the sample as layers are ion-bombarded away. This is not unusual as most chemical vapor deposited fibers have some oxygen in them. For example, analyses of electronic grade, high purity Si_3N_4 fibers in this laboratory have always shown at least 2% oxygen to be present.

During the course of these experiments one spurious result was obtained and seem worth mentioning here. During the measurements of the peak to peak heights of B and N while bombarding with electrons, a change in ratio was observed, indicating a possible desorption of a small amount of N. This experiment was repeated several times but could not be reproduced. Two possible explanations are first, that something in the measurement process changed, electronically in the Auger spectrometer or controller, chemically in the vacuum system or secondly, that the BN is not completely homogeneous and we were fortunate enough to be located on a susceptible region. We lean toward the former explanation as we performed many subsequent measurements with no repeat of this result.

It is possible to obtain a little information about the charging of the BN. The beam was directed to the edge rather than the basal planes. At normal incidence, charging occurred to a great extent. For example, the Auger spectrum was shifted about 800 volts for a 3KeV beam at normal inci-

dence, indicating a charging of the sample to approximately 800 volts. Ion-bombardment also produced severe charging but the degree of such charging was not measured. The effects of the ion beam seemed very slow to decay. In some cases Auger spectra of ESCA spectra could not be taken for many hours following ion-bombardment.

Ion-bombardment, irrespective of charging, does easily sputter the surface. Very good secondary ion mass spectra were obtained using 2KeV incident argon or xenon ions and both + and - sims spectra were taken. No unexpected elements were present in these spectra.

To complete this work some analyses of components of TWT's that have undergone long term testing should be undertaken. There may be appreciable amounts of B and N (or BN) on these surfaces. This may not be the result of electron bombardment, however, but may be due to ion-bombardment or from unexpected heating of the rods in certain places. The effects of BN on the secondary emission coefficients of copper collectors should probably be investigated as well.

Finally, studies such as the ones performed herein should be conducted on all materials planned for use in TWT's. AlN has been suggested for such use and should be investigated to determine its behavior. Diamond is already known to convert to graphite upon electron bombardment but whether this will be detrimental is not known.*

*It has recently been brought to our attention that graphitization of the surfaces of diamonds during electron gun operations prevents their use as insulators for shadow grids in certain microwave tube devices (Reference 20). Whether similar results would occur for helix support applications is not known.

SECTION V

CHARACTERIZATIONS OF NONEVAPORABLE GETTERS FOR TWT APPLICATIONS

1. INTRODUCTION

Studies of the activation of a ST-171 nonevaporable getter manufactured by SAES Getter, Inc. were completed in this work unit. This work was undertaken because this getter had been proposed for use in a DSCS TWT. The getter is purportedly a mixture of zirconium metal powder and graphite, which has a wound heater embedded in it for indirect heating. The nonevaporable getter is activated to reduce the residual gases in the TWT. Residual gases in a TWT will have several deleterious effects. The gases will interfere with the electron beam and cause the electron beam to scatter and defocus. Conversely, the electron beam will ionize the gases and the ions will back-stream to the cathode and sputter the cathode surface causing emission current degradation.

A series of experiments were conducted to follow the changes in getter surface chemistry and to determine the types and relative quantities of gases evolved during activation. From this data we were to determine the optimum conditions for use in the TWT, and to suggest procedural changes in TWT processing if necessary.

2. EXPERIMENTAL PROCEDURE

The experiments on the getters utilized XPS to follow the changes in surface chemistry (Reference 2) and line of sight residual gas analysis (LOSRGA) (Reference 21) to determine the types and relative quantities of gases evolved. The getters were mounted in the vacuum chamber on the specimen manipulator so that they could be positioned in line of sight to the UTI, Inc. Model 100C Residual Gas Analyzer and also be rotated to the

focal point of the Physical Electronics Industries Model 550 ESCA/SAM Spectrometer, a double pass CMA. After baking the vacuum chamber at 250°C for 4 hours the pressure attained overnight was 2×10^{-10} torr. The temperature of the getter was determined by means of a heater current versus temperature curve supplied by SAES, Inc.

Each experiment began by taking XPS data on the as-received getter. The getter was then positioned in front of the RGA in order to outgas in line of sight during the temperature increase, then positioned back in front of the spectrometer for more XPS data. At each temperature increase this process was repeated. Evidently the heater was inductively wound because we had magnetic field problems when the heater current was applied. Therefore the temperature was not maintained while the XPS data was being taken.

Activation of the nonevaporable getter was accomplished in several ways. In one set of experiments the getter was slowly heated in steps of heater current to 900°C. In another set of experiments the getter was flashed to 900°C, i.e., the heater current was immediately set to the 900°C equivalent. A third set of experiments was set up to closely simulate the treatment the ST-171 nonevaporable getter would receive if installed in a TWT during the preprocessing and processing steps.

3. EXPERIMENTAL RESULTS

a. LOSRGA

The set of experiments in which the getter heater current was slowly increased was set up to determine at what temperature, which species of the gases were being evolved. The gas evolution was monitored by taking RGA data for 0 to 60 amu. The initial pressure increase occurred between 200°C and 300°C, and the pressure kept increasing to the 900°C temperature

maximum. Hydrogen was the major constituent of the gases evolved, by about a factor of 10, with lesser amounts of water, carbon monoxide and carbon dioxide.

In the next set of experiments, the getter was flashed to 900°C for five minutes. We were attempting to achieve full activation according to SAES, and to monitor both the gases evolved and the total pressure rise. It should be remembered that a 300 liter/sec ion pump as well as a titanium getter were operating throughout these experiments. Thus this pressure rise is not indicative of expected behavior in the small volume of a sealed tube. The gases were monitored by multiplexing the peaks due to H_2, H_2O, CO, and CO_2 at masses 2, 18, 28, and 44 respectively. The outgassing characteristics are shown in Figure 12, along with an estimate of the partial pressures for the gases shown. The partial pressures were calculated using sensitivity factors supplied by the RGA manufacturer and using the total pressure (measured with the RGA in the total current mode) and applying gauge sensitivity factors (Reference 22) for the various major species detected. Both calculations gave similar results.

The last set of experiments, the tube processing simulation, gave results similar to the other two sets of experiments. In this case the sequence was as follows:

a) heat to 450°C hold for 16$\pm$ 1 hr

b) heat to 500°C hold for 1/2 hr

c) heat to 600°C hold for 1/2 hr

d) back to 500°C hold for 1/2 hr

e) heat to 700°C hold for 1 hr

f) allow to cool and expose to dry N_2 and air

g) repeat a and b

The outgassing for the temperature rise to 600°C (a,b,c above) is summarized in Figures 13 a and b. At each temperature increase, H_2 is the major constitutent of the gases evolved, with lesser amounts of CO_2, CO, and H_2O.

b. XPS

Surface analysis measurements were also made on these getters using the XPS technique. The results of the three different sets of experiments were similar, therefore, only one set of results will be presented. A wide XPS scan of the getter in its as-received condition is shown in Figure 14. The elements present are Zr, C, and O. High resolution scans of the C1s and Zr3d transitions, shown in Figure 15 and 16, suggest that the Zr was present on the surface as ZrO_2 and that the carbon was largely in the graphite or hydrocarbon form (the difference in energy between the C1s peaks for graphite vs. most C-H forms is not measurable.) As the temperature of the getter was increased, the relative chemical constituents of the surface changed as shown in Figures 14, 15, and 16. The wide scan, after activation in Figure 14, shows an increase in signal due to Zr and a decrease in signal due to O and C. The high resolution scan of C, after activation in Figure 15, shows a second peak and the high resolution scan of Zr, after activation in Figure 15, shows a peak shift. The two components of the carbon peak are identified as graphite and as a carbide of Zr. The sample shows some charging behavior which will shift the apparent energies of the peaks. Therefore, the C1s graphite peak is assigned its known value of 284.6 eV (Reference 23) and all other peak energies were corrected to this standard. Such a procedure shifts the $Zr3d_{5/2}$ peak to 179.1 eV, a value very close to that reported for Zr metal (Reference 23). XPS data after exposure to air are also shown for C and Zr in Figures 15 and 16. The

principal change was the increase in C and O. As expected little or no N is absorbed, since chemisorption of H_2O, CO_2 and O_2 is much stronger than N absorption. The high resolution scans of Zr shows several chemical states for Zr, probably due to ZrO_2, ZrC, and the underlying Zr metal. The high resolution scan of C also suggests carbon exists in several chemical states. The last set of XPS spectra in Figures 15 and 16 for a reheat of the getter are again similar to those of the activated getter. XPS spectra were also taken at other temperatures, with data for the Zr peak summarized in Table 2. The results of these data show the shift in the Zr peak from that of a ZrO_2 value toward that of a Zr metal value during the activation process.

4. CONCLUSIONS

The following points can be concluded from these experiments:

a) The activation of the getter accomplished by some solid-state chemical reaction which produces a near-metallic Zr surface.

b) Residual gases given off when activating the getter are principally H_2 with some H_2O, CO and CO_2 appearing as well.

c) The pumping of such gases as CO, CO_2 and H_2O should be relatively permanent in that ZrO_2 and ZrC will be formed by reaction of clean Zr metal with these gases. The bonds formed to Zr are sufficiently strong so as to break C-O and H-O bonds even at room temperature. Since hydrogen diffuses very rapidly in Zr, bulk dissolution is also likely (References 24 and 25).

SECTION VI

FAILURE ANALYSIS OF TWT COMPONENTS

1. INTRODUCTION

A variety of failure analyses and component characterization on production TWT's and piece parts for these TWT's for the DSCS II and III programs were completed in this program. Some of the more significant of these efforts will be summarized in this section.

2. EXPERIMENTAL PROCEDURE

Oxide cathodes intended for use in long term applications such as in satellite communication systems are usually comprised of a Ba-Sr (and sometimes Ca) oxide coating on a nickel alloy support. The cathode nickel is a special alloy containing, among other elements, such metals as Mg or Zr which are added to serve as long term activators (Reference 26). The exact role of the Zr of Mg is not thoroughly understood nor is the ultimate destiny of the Zr of Mg after long term (years) operation, i.e., it is oxidation, surface or interface segregation, or Ba diffusion into the nickel followed by chemical combination to form Ba zirconates, etc. Such questions are themselves interesting research topics. It is known, however, that some significant fraction of the activator must be present in the metallic state in order to be effective.

A problem was encountered with one batch of cathode nickel being used in production in DSCS tubes which suggested that the Zr present in about 0.01% level in the Ni was already in the oxidized state. To determine if indeed this was the case, several pieces of the cathode nickel alloy prepared in various ways were analyzed using x-ray photoelectron spectroscopy. Supplementary investigations were preformed on pure Zr metal and on ZrO_2 layers on Zr metal to determine the binding energy shifts to be expected. Additionally, it was found that argon ion-bombardment

did not efficiently reduce the oxide back to the metallic state as is the case with many other metal oxides. It appeared that ion-bombardment could be used to remove surface layers of Ni and Zr which themselves were certainly oxidized form various environmental exposures to reveal the chemical states of the bulk elements. It was also found that Zr in the metallic state was very reactive to residual gases in the vacuum system but that only a very thin oxide formed during the times necessary to make XPS measurements. Thus, the escape depth of the photoelectrons being measured and hence the sampling depth into the surface will be great enough (10-20 A° or more) so that much of the signal will come from bulk Zr atoms unaffected by residual gas contamination.

The results of these examinations can be summarized by reference to Figure 17 which shows the Zr 3d peaks from an ion-bombarded cathode nickel surface. Using the earlier standards for Zr-metal and ZrO_2 one can unequivocally identify the overwhelming bulk of the Zr present as being in the oxidized form.

3. INVESTIGATIONS FOR LEAKS IN LIFE TESTED TWT's

A TWT that was undergoing long term life testing showed slow degradation of cathode activity throughout life. The tube passed its design goal of 50,000 hours operation, but the degradation was still a matter of concern. It was suspected that a small leak in the vacuum envelope was accidently penetrated so that it was not possible to do a residual gas analysis to determine the presence of atmospheric gases, primarily nitrogen using such methods as described by Graven, Gilmartin and

Wachi (Reference 27). The tube was subsequently dissected and various electrodes and collector components were sectioned. It was felt that if a leak existed during long-time tube operation that nitrogen would be a principal gaseous component but more importantly would tend to be ionized by the high current density electron beams present. This ionized nitrogen would be implanted into selected electrode or collector surfaces but in nonuniform distributions dependent on the electrical potentials and their locations within the tube. First investigations using scanning AES to measure nitrogen concentrations on the electron gun components gave essentially negative results. Later measurements on the collector surfaces, however, did show the presence of significant amounts of nitrogen. The collector is made of copper which does not normally absorb molecular nitrogen to any great extent. Thus, any nitrogen present must either have been implanted or reacted by being ionized or in an excited state. Significantly, the concentration of the nitrogen along the surface of the collector was not uniform but varied as shown in Figure 18 in a manner to be expected from the known potential distribution in the collector region. Although this information is not totally conclusive it is strongly suggestive of a small leak during long-term life test of the tube, very likely in a metal-ceramic braze in the collector region.

4. DETERMINATION OF THE DECOMPOSITION TEMPERATURES OF ALKALINE EARTH CARBONATES USED IN OXIDE CATHODES

The alkaline earth oxides in the coating on oxide cathodes are not applied to the cathode support surfaces as oxides but rather are applied in the form of carbonate powders, usually in some sort of cleanly degradable organic binder.

This is done because the oxides are hygroscopic and tend to form hydroxides which will decompose, but unwanted sintering of the coating usually occurs as well. The carbonates are not so hygroscopic and tend to decompose according the reaction:

$$BaCO_3 \rightarrow BaO + CO_2 \uparrow$$

The exact temperature at which this reaction proceeds at a reasonable rate is thus important because tubes are baked out during vacuum processing to the highest temperatures possible consistent with the materials of tube construction. If the decomposition of the carbonates occurs during tube bakeout it is possible that gaesous poisoning or sintering of the cathode coating will occur. It was necessary, therfore, to make relatively precise measurements of the partial pressures of CO_2 over an unactivated cathode as a function of temperature while pumping in ultra-high vacuum. Measurements were made of both double carbonates (Ba-Sr CO_3) and triple carbonates (Ba-Ca-Sr-CO_3). A typical residual gas analysis is shown in Figure 19. It can be seen that the partial pressure of CO_2 begins to rise slightly at temperatures of approximately 570°C. The decomposition proceeds very rapidly (two or three orders of magnitude increase in the partial pressure of CO_2) at temperatures in the 650 to 700°C range. At 700 to 750°C the decomposition is essentially complete. These results seemed to be essentially the same regardless of whether a double or triple carbonate coating was applied.

5. DISTRIBUTIONS OF Ba AND Sr ACROSS THE SURFACE OF A LIFE TESTED OXIDE CATHODE

The double and triple carbonates that are applied to nickel substrates in the fabrication of oxide cathodes may be either mixtures of the individual powders or may be so-called misch-crystals which are co-precipitated forms of the carbonates. The mixtures will, of course, be

somewhat nonuniform initially on a scale the size of the particle dimensions. During operation over a long period of time at elevated temperatures it is possible that a homogenization may occur. To test this hypothesis a series of SAM measurements were made on an oxide cathode that had been life tested in a tube environment for some 50,000 hours. The results of these measurements may be seen in Figure 20 which displays the surface lateral distributions of the Ba and Sr on this cathode. It can be readily seen that the distributions are quite inhomogeneous indicating that limited mixing has occurred. There are displayed in this figure - two maps for the Sr, one the high energy transition at 1649 eV and a low energy transition at 110 eV. It is well known (Reference 28) that the electron mean free path, λ, in a solid is a strong function of electron energy. The higher transition is expected to have a $\lambda \sim 25$ A° while the lower energy one would have a $\lambda \sim 5$ A°. This difference in λ allows one to obtain some information on depth distributions of a given element as the lower energy transitions will be more surface localized while the higher energy transition reflects more bulk-like concentrations. These differences are readily apparent in Figure 20, showing areas of high surface Sr concentrations and other areas where the Sr distribution is similar for both the high and low energy transitions indicating a uniform distribution with depth.

6. CONTAMINATION OF A DISPENSER CATHODE DURING TUBE OPERATION

High power ECM TWT's frequently utilize a grid placed close to the cathode to control pulsed tube current. A tube of this type was found to have a low cathode emission current. Cathode poisoning, perhaps by a titanium control grid, was suspected. The tube was disassembled and the cathode mounted for SAM analysis. The results of these measurements are shown in Figure 21. The distribution of Ti across the surface is in a pattern expected from contamination from a Ti grid spaced nearby and

deposited onto the cathode either by sputtering or by evaporation. Sputtering might occur if the tube pressure rose to a high value whereas evaporation would occur if the grid cathode spacing were too close.

7. SUMMARY

The failure analysis investigations reported in this section show the many ways in which surface analytical techniques can be used to solve a variety of production and design problems. The applications are limited only by the resourcefulness of the investigators but require a judicious use of the right techniques to the problem at hand. These results demonstrate very clearly the complementary nature of SIMS, ESCA, SAM, Auger depth profiling and the like and point up the need to have this variety available as required. Close collaboration between the surface analyst and the tube engineer is clearly indispensable as well.

REFERENCES

1. "Handbook of X-ray and Ultraviolet Photoelectron Spectroscopy", D. Briggs, Ed., Hyden & Son Inc., Philadelphia, PA, 1978.

2. "Methods of Surface Analysis", A. W. Czanderna, Ed., Elsevier Scientific Publishing Co., New York, N.Y., 1975.

3. E. B. Hensley, J. Appl. Phys. 32, 301 (1961).

4. D. W. Maurer, Bell Telephone Tech. J., 46, 2363 (1967).

5. R. Dominguez, H. Doolittle, P. Varadi, LeVide, 118, 289 (1965).

6. P. Zahn in Electronics and Electron Physics, I. Martin, Ed., Academic Press, New York, N.Y., Vol. 26, p 211, 1968.

7. G. A. Haas in "Methods of Experimental Physics", Academic Press, New York, N.Y., Vol 4, p. 1, 1960.

8. R. W. Jenkins, Vacuum 19, 353 (1969).

9. G. A. Haas, A. Shih, and R. E. Thomas, J. Appl. Phys. 47, 5400, (1976).

10. G. A. Haas, A. Shih, and R. E. Thomas, Applications of Surf. Sci., 2, 293 (1979).

11. W. V. Lampert, B. C. Lamartine, K. D. Rachocki, and T. W. Haas, Applications of Surface Science, to be published.

12. B. C. Lamartine, W. V. Lampert, K. D. Rachocki, and T. W. Haas, Proceedings of International Conference on X-ray Processes and Inner Shell Ionization, to be published.

13. G. E. Moore and H. W. Allison, J. Chem. Phys. 23, 1609 (1955).

14. R. Forman, Applications of Surface Sci., 2, 258 (1979).

15. G. Schion, Acta Chem. Scand. 27, 2623 (1973).

16. S. W. Gaarenstroom and D. N. Winograd, J. Chem. Phys. 67, 3500 (1977).

17. R. W. Springer and B. C. Lamartine, to be published.

18. W. L. Baun, Applic. Surf. Sci. 4, 375 (1980).

19. T. W. Haas, J. T. Grant, and G. J. Dooley III, J. Appl. Phys. 43, 1853 (1972),

20. G. Dohler, Northrup Corp., Private Communication.

21. B. C. Lamartine, W. V. Lampert, T. W. Haas, "AES-RGA Investigations of Various Type Cathodes During Activation in Ultrahigh Vacuum", Submitted to App. Surf. Sci.

REFERENCES (Concluded)

22. "The Precision Mass Analyzer" the Technology International, U.S.A. 1979, Appendix B, pp. 1-6.

23. G. E. Muilenberg (Editor) "Handbook of X-ray Photoelectron Spectroscopy" Perkin-Elmer Corp., Phusical Electronics Div., U.S.A., 1979, pp 100-101.

24. J. F. Hon, J. Chem. Phys., 36, 759 (1962).

25. E. A. Gulbransen and K. F. Andrews, J. Electrochem. Soc. 101, 560 (1954).

26. F. M. Wachi, N. Marquez, and J. R. Shepherd, SAMSO-TR-77-183.

27. W. M. Graven, D. W. Gilmartin, and F. M. Wachi, Aerospace Corporation Report TOR-0079 (4402) -4, Vol 1.

28. C. J. Powell, Surface Sci., 44, 29 (1974).

29. R. D. Perkins, Practical Theory and Operation of Traveling Wave Tubes, R&L Technical Publishers, San Jose, Calif., 1973.

TABLE 1

RESULTS OF ELECTRON SPECTROSCOPIC MEASUREMENTS ON
Ba and Ba COMPOUNDS

Energy values on XPS measurements are referred to an MgK line at 1253.6 eV and values given are accurate to ±0.2 eV. Details on materials are included in the text. "APES" refers to the Auger-Photoelectron Energy Separation of the Binding Energy Scale for the Ba $3d5/_2$ to $M_4N_{4,5}N_{4,5}$ Auger line. All measurements are referred to Au 417/2 at 83.8 eV.

Material	$3d_{5/2}$ B.E.	$M_4N_{4,5}N_{4,5}$	APES
Ba (thick film)	779.8	651.7	128.1
Ba on W (monolayer)	779.5	651.5	128.0
Ba-O-W	779.5	653.5	126.0
O-Ba-W	779.0	654.4	124.6
BaO-W (thick film)	*	654.4	124.6
$BaWO_4$ (cathode)	*	*	124.0
$BaCO_3$ (bulk powder)	*	*	123.9
BaO (bulk powder)		*	123.6

*No value reported due to suspected sample charging.

TABLE 2

ROOM TEMPERATURE ENERGIES OF Zr 3d PHOTOELECTRON LINES VS. ACTIVATION TEMPERATURE OF ST-171 GETTER REFERENCED TO C1s (GRAPHITE) AS 284.6eV

Condition	Zr 3d (eV)
Not Activated	182.1
Flashed	179.1
Not Activated	182.5
At 450°C (Hot)	179.4
After 600°C	179.3
Air Exposure	182.3
After 500°C	179.5

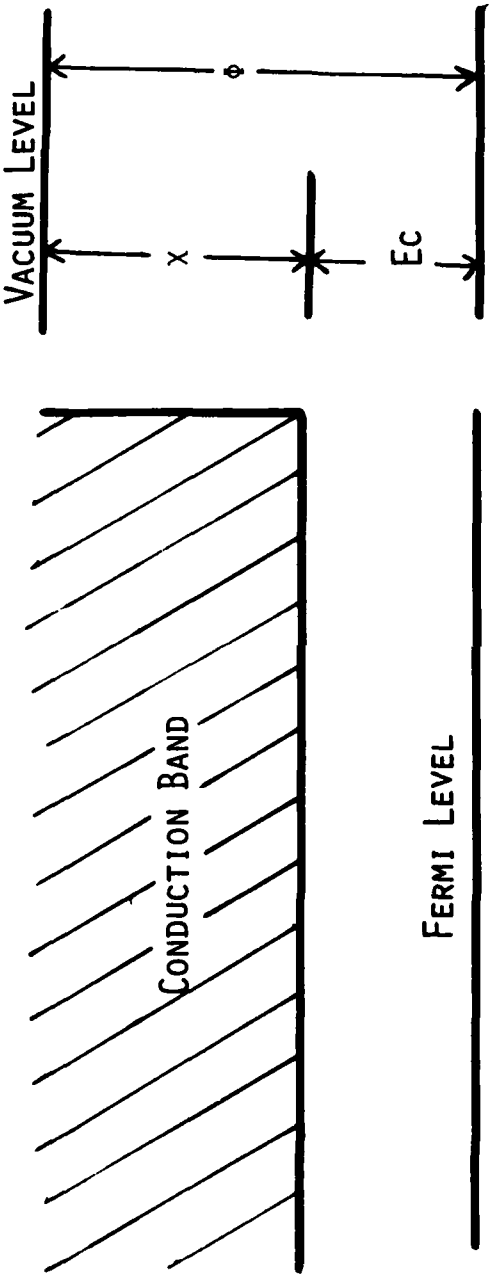

Figure 1. Simplified Energy Level Diagram for a Semiconductor Such as BaO Illustrating Relationship of Work Function to Electron Affinity and Position of the Conductor Band Edge E_c.

SANDWICH MODELS

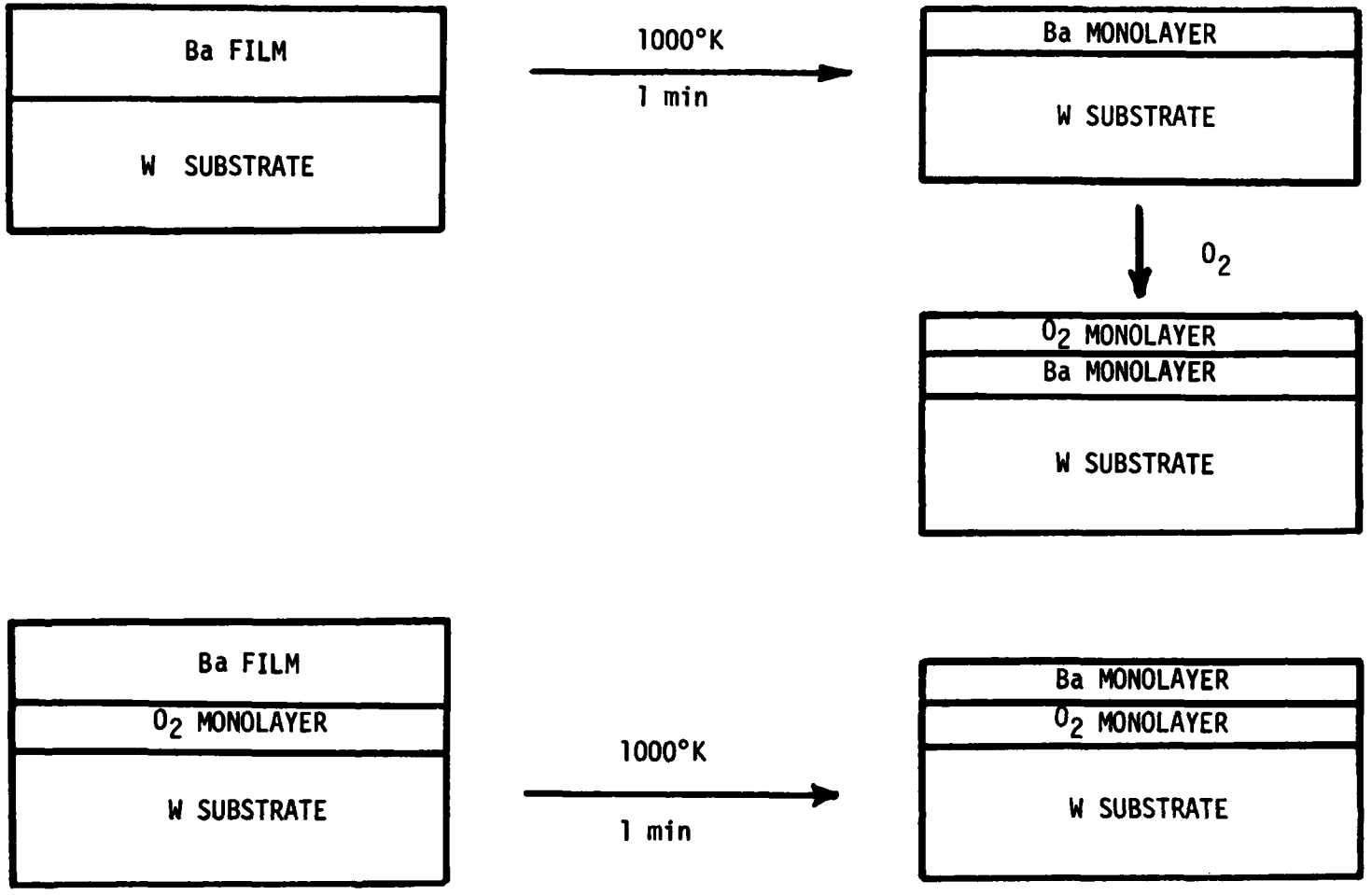

Reference: R. Forman, J. Appl. Phy., 47(1976) 5272 and G. E. Moore and H. W. Allison, J. Chem. Phy., 23 (1954) 1609.

Figure 2. Schematic Description of Techniques Used to Produce Multilayer and Monolayer Sandwich Structures of Ba on W, Ba on O on W, and O on Ba on W.

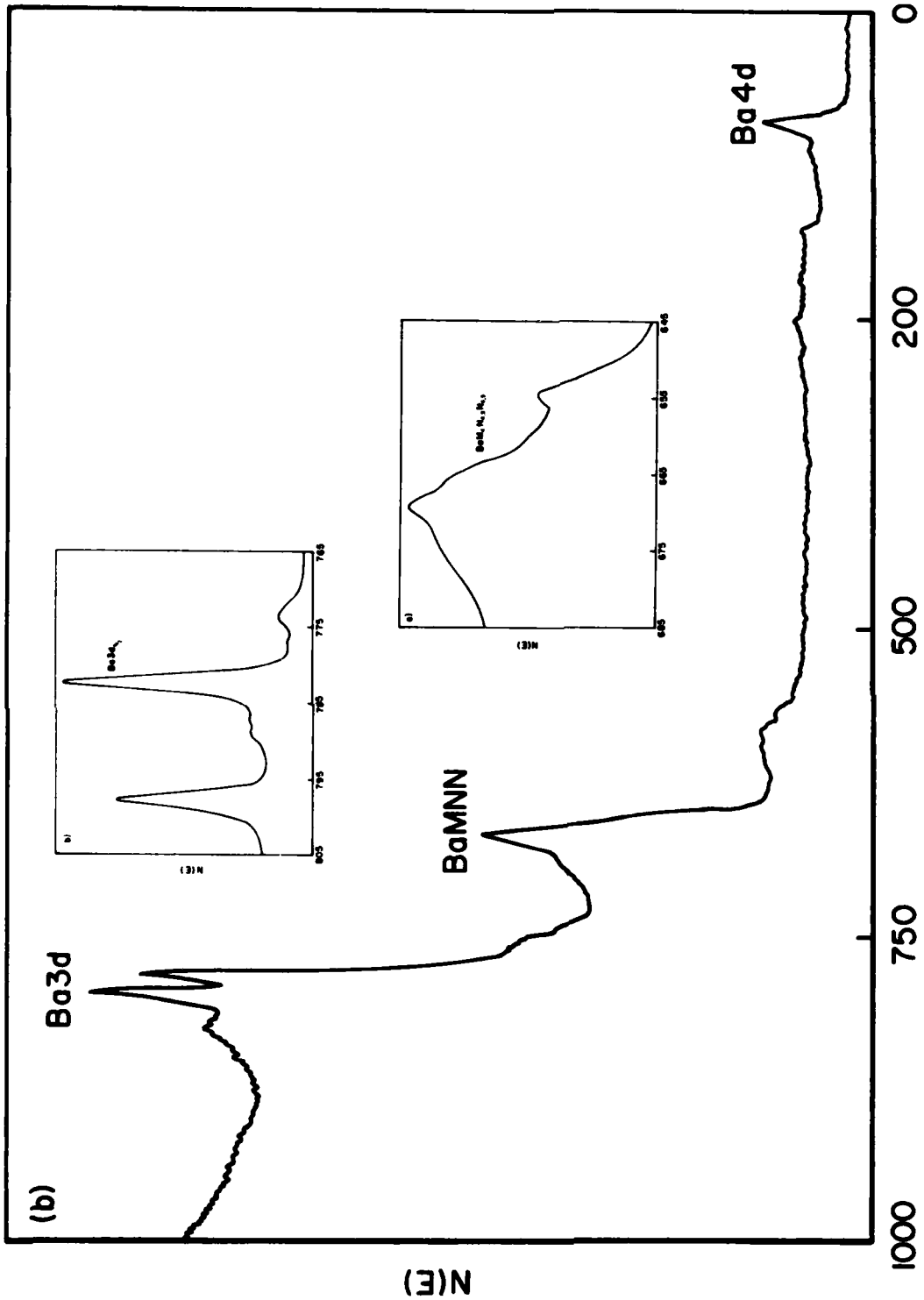

Figure 3. Wide Scan of Thin Ba Metal Film on Cleaned W Foil Illustrating Principle of the Auger-Photoelectron Energy Separation Measurements. Inserts Show Two High Resolution Energy Scans of the Ba 3d Photoelectron Energy Region and the Ba MNN X-Ray Excited Auger Feature. The APES Used in This Work Monitors ^{4}S Energy Separation.

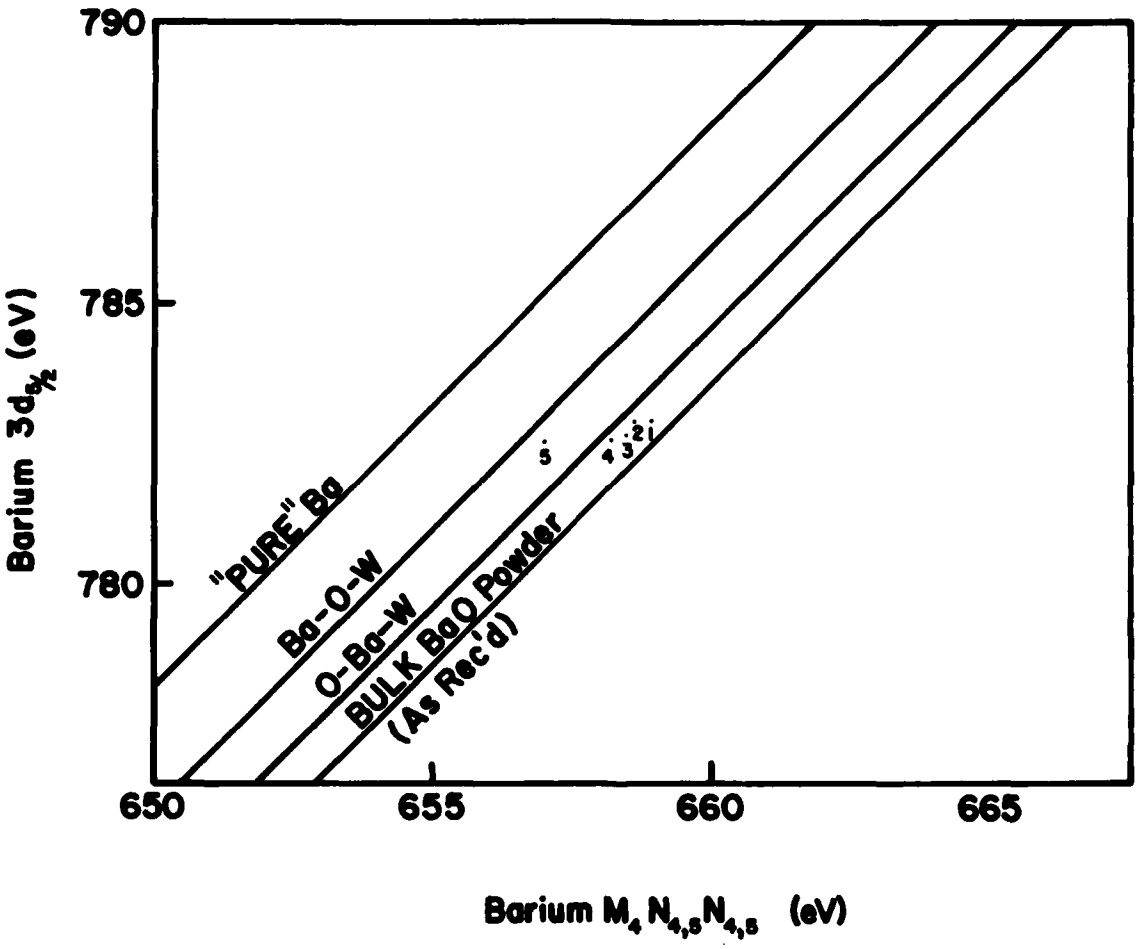

Figure 4. APES Plot for Barium and Some of its Compounds. Charging Merely Displaces Data Points Along a Given Line While a Chemical Shift Upon Compound Formation Causes the Points to Cross APES Lines. Most of These Progressions Were Nearly Horizontal Because of the Small Influence of the Ba $3d_{5/2}$ Line Energy Changes. Numbered Points Show Changes in the Ba APES from a Dispenser Cathode During Activation. The Temperatures at which the Data Were Taken are 1) Room Temp., 2) 50°C, 3) 165°C, 4) 400°C, 5) 650°C.

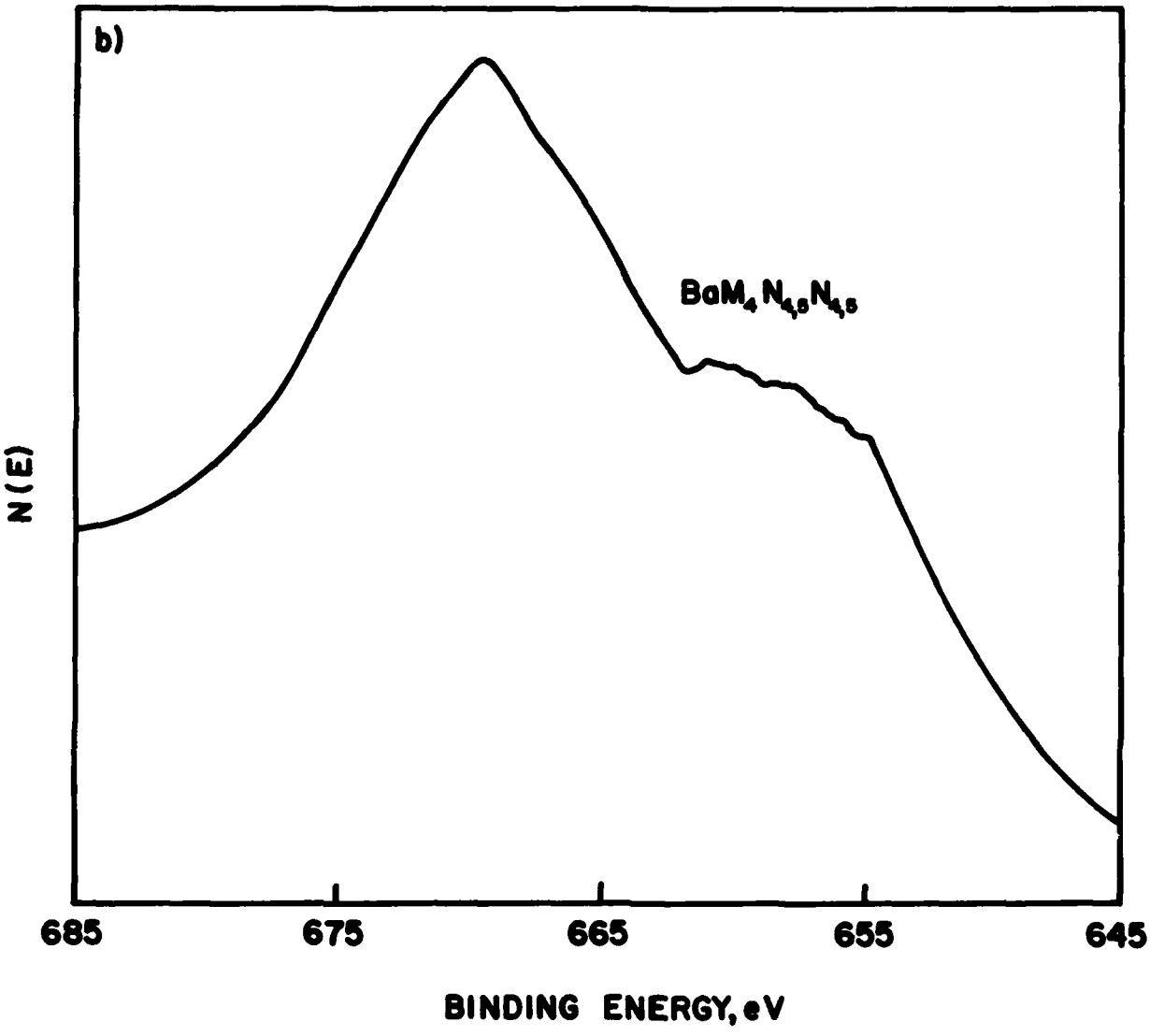

Figure 5. X-Ray Excited Ba MNN Feature from a Fully Activated Dispenser Cathode. Note Loss of Peak Definition of the Low Binding Energy Side of the Feature.

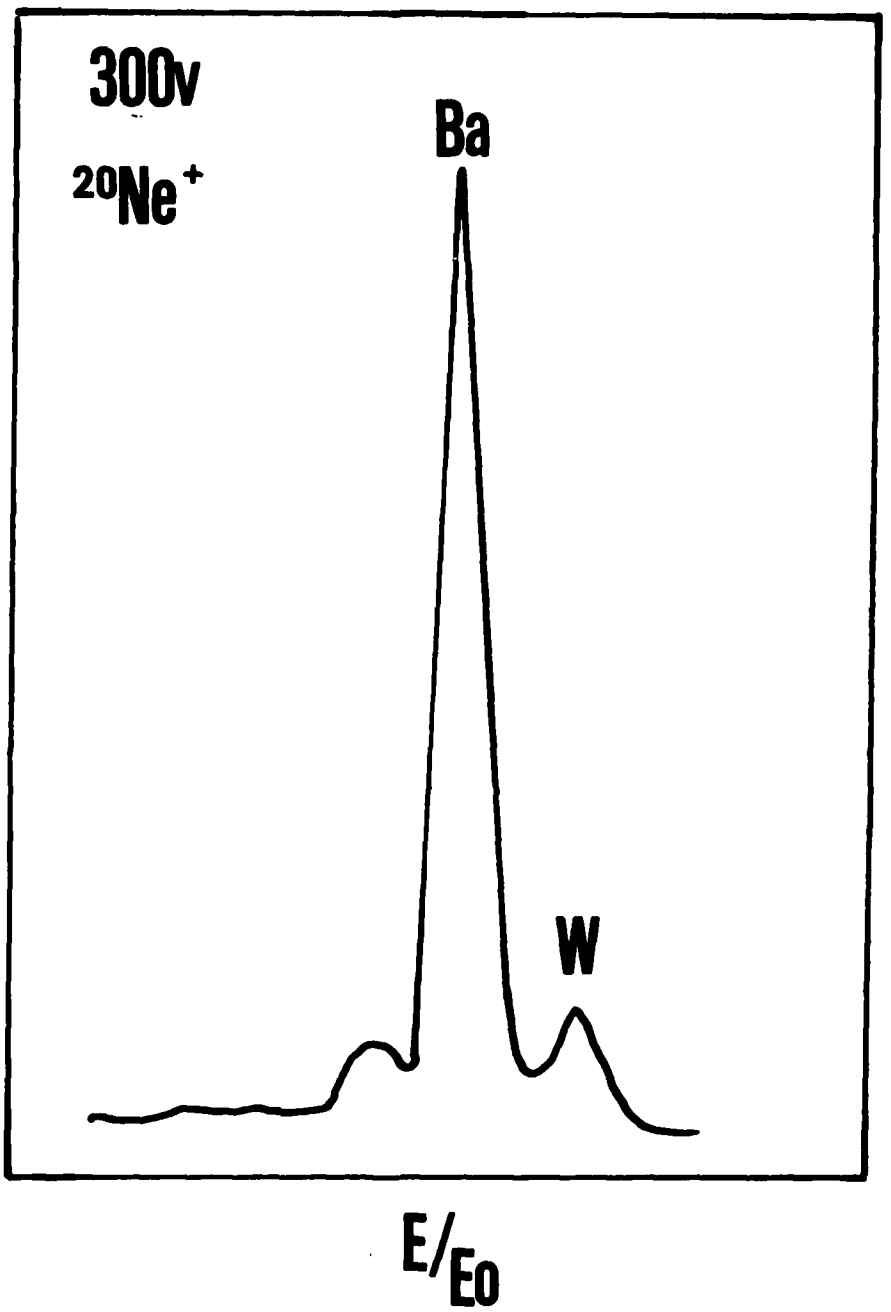

Figure 6. Low Energy (300eV) Ne+ Ion Scattering Spectroscopic Measurements of a Fully Activated Dispenser Cathode. Ba is the Dominant Scattering Atom on the Cathode Surface.

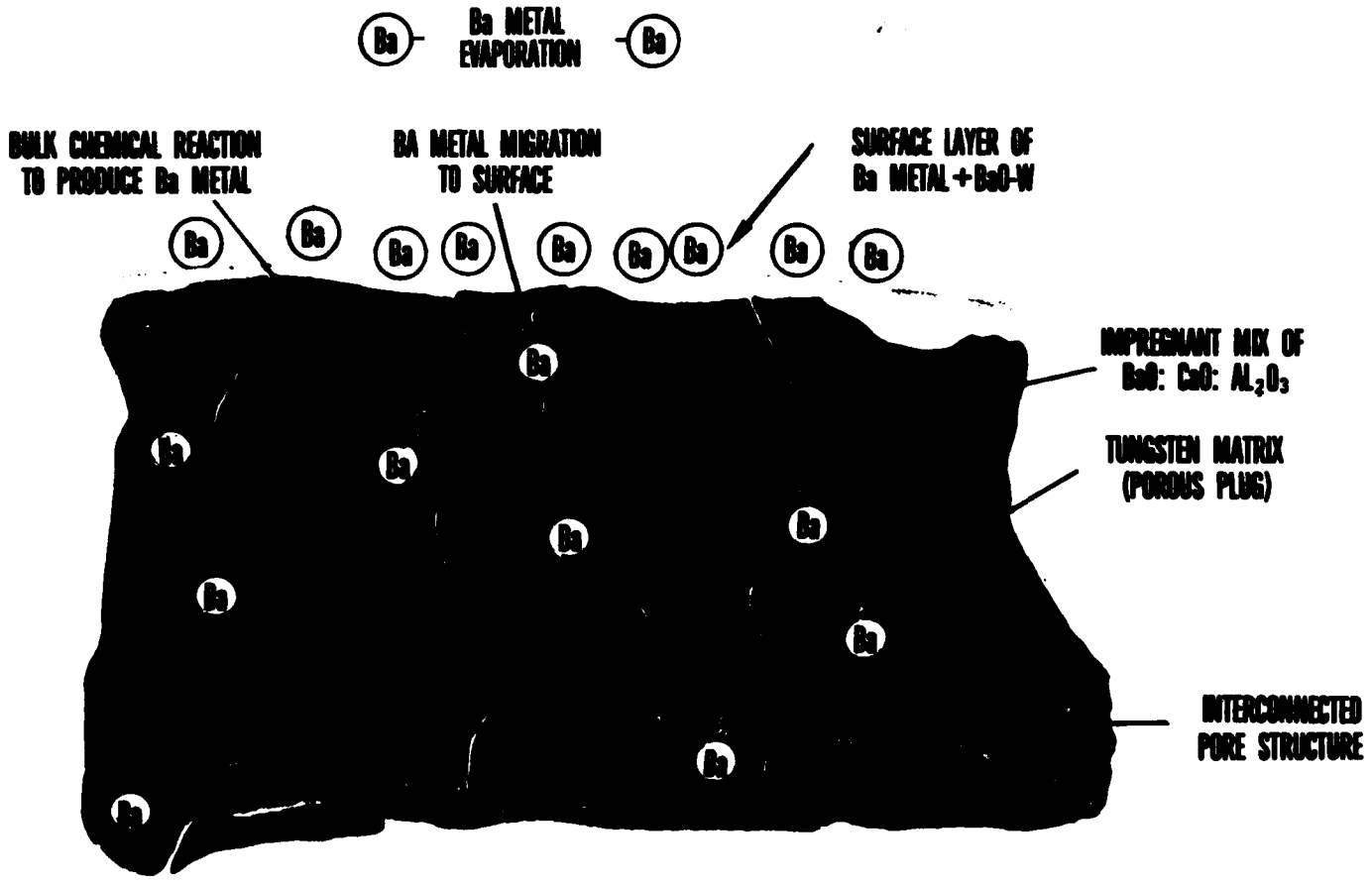

MODEL OF ACTIVATED IMPREGNATED TUNGSTEN DISPENSER CATHODE

Figure 7. Schematic of Impregnated Tungsten Dispenser Cathode after Activation and During Operation. Ba Metal is Generated in the Bulk of the Porous Plug, Migrates to the Surface and Absorbs on a Partially Oxidized Tungsten Surface.

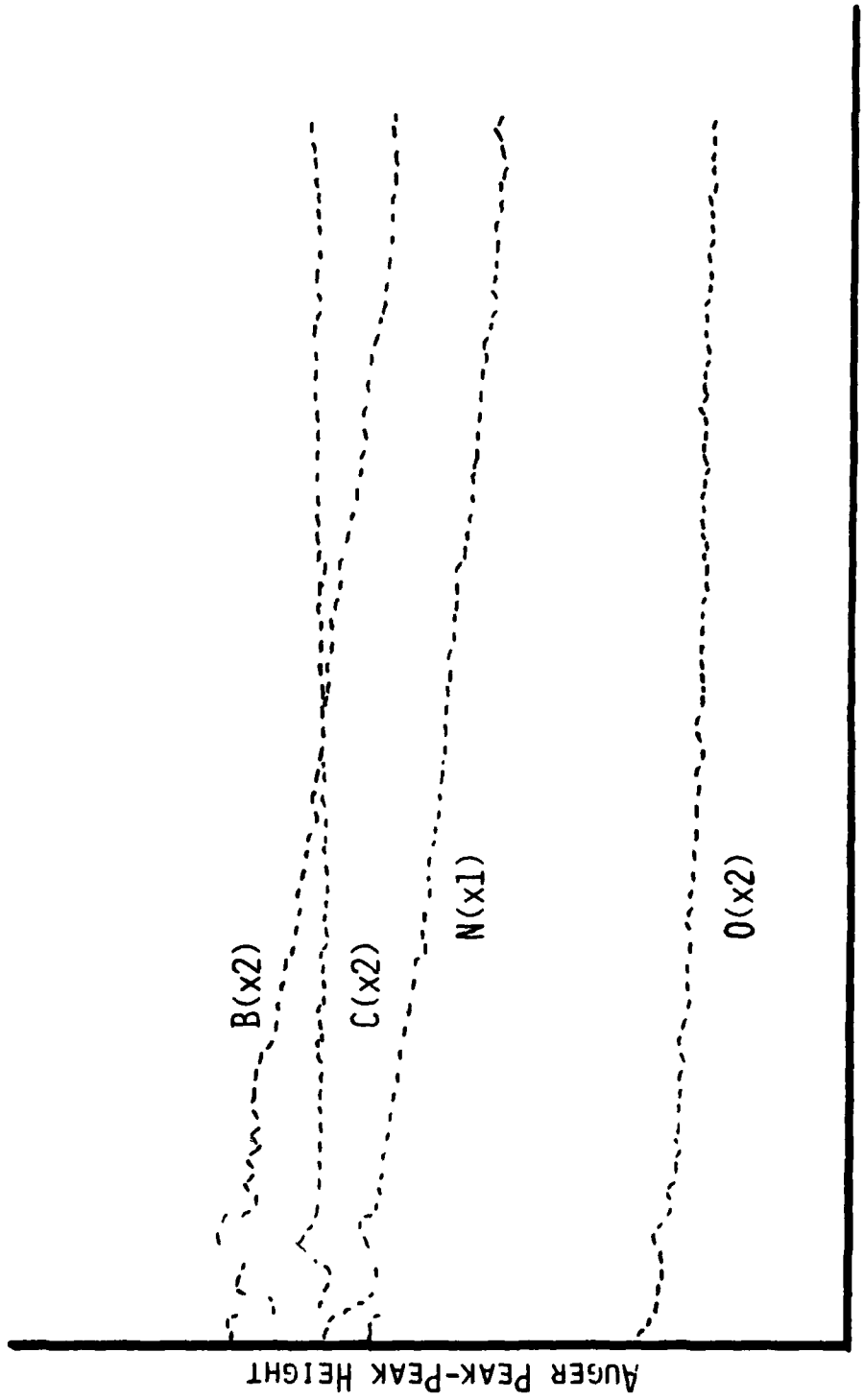

Figure 8. A Plot of the Auger Peak to Peak Heights for Boron and Nitrogen as a Function of Time for a BN Sample Undergoing Electron Bombardment.

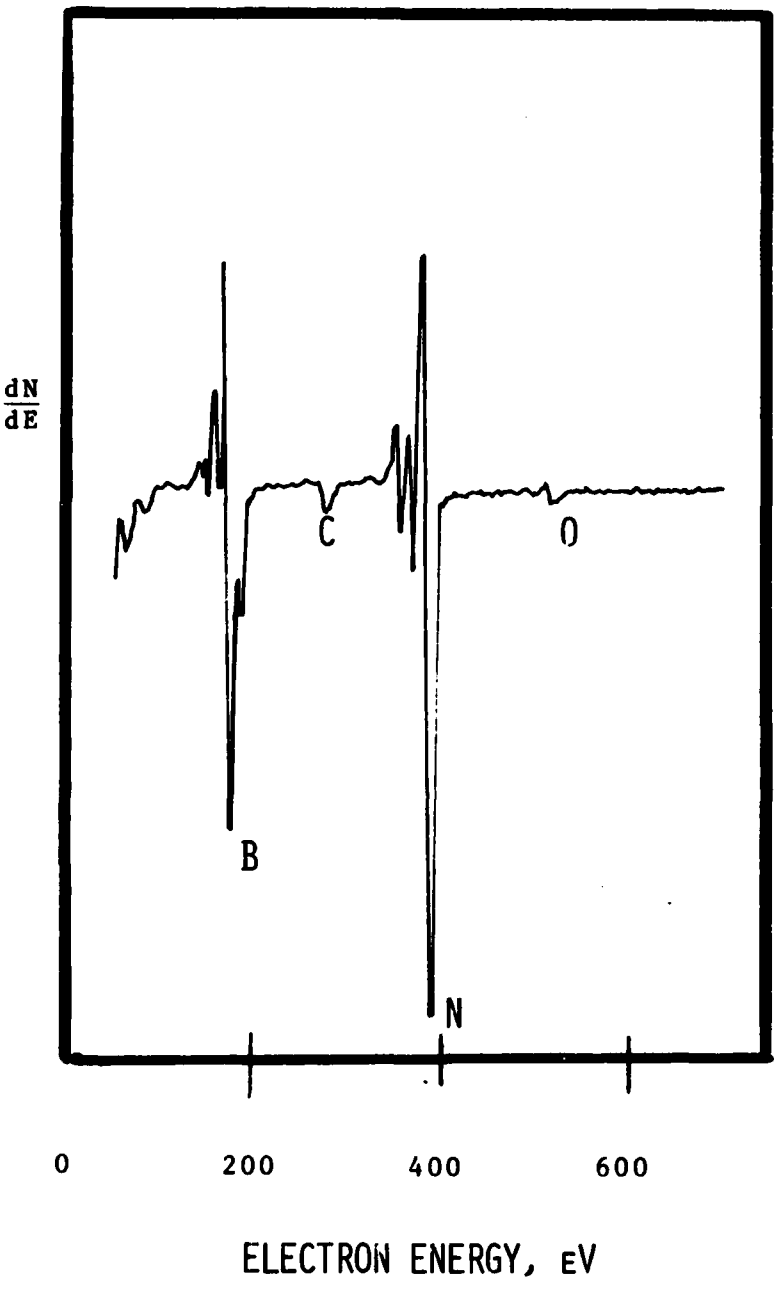

Figure 9. Auger Peak Shapes for the B KLL and N KLL Auger Transitions from a BN Sample.

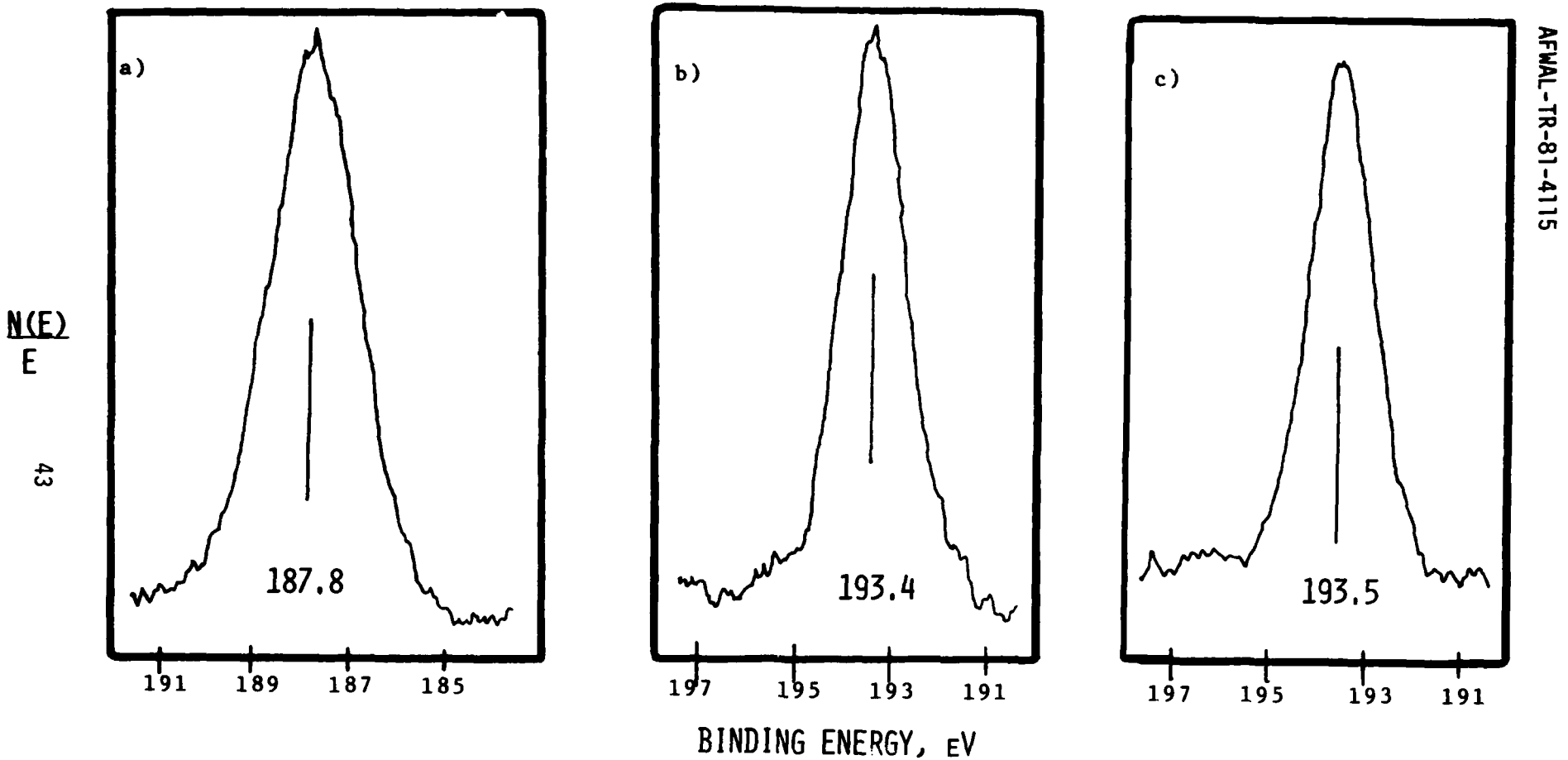

Figure 10. ESCA Spectra of the B 1s Peaks for (a) Pure B Metal (b) BN Before Electron Bombardment and (c) After Electron Bombardment.

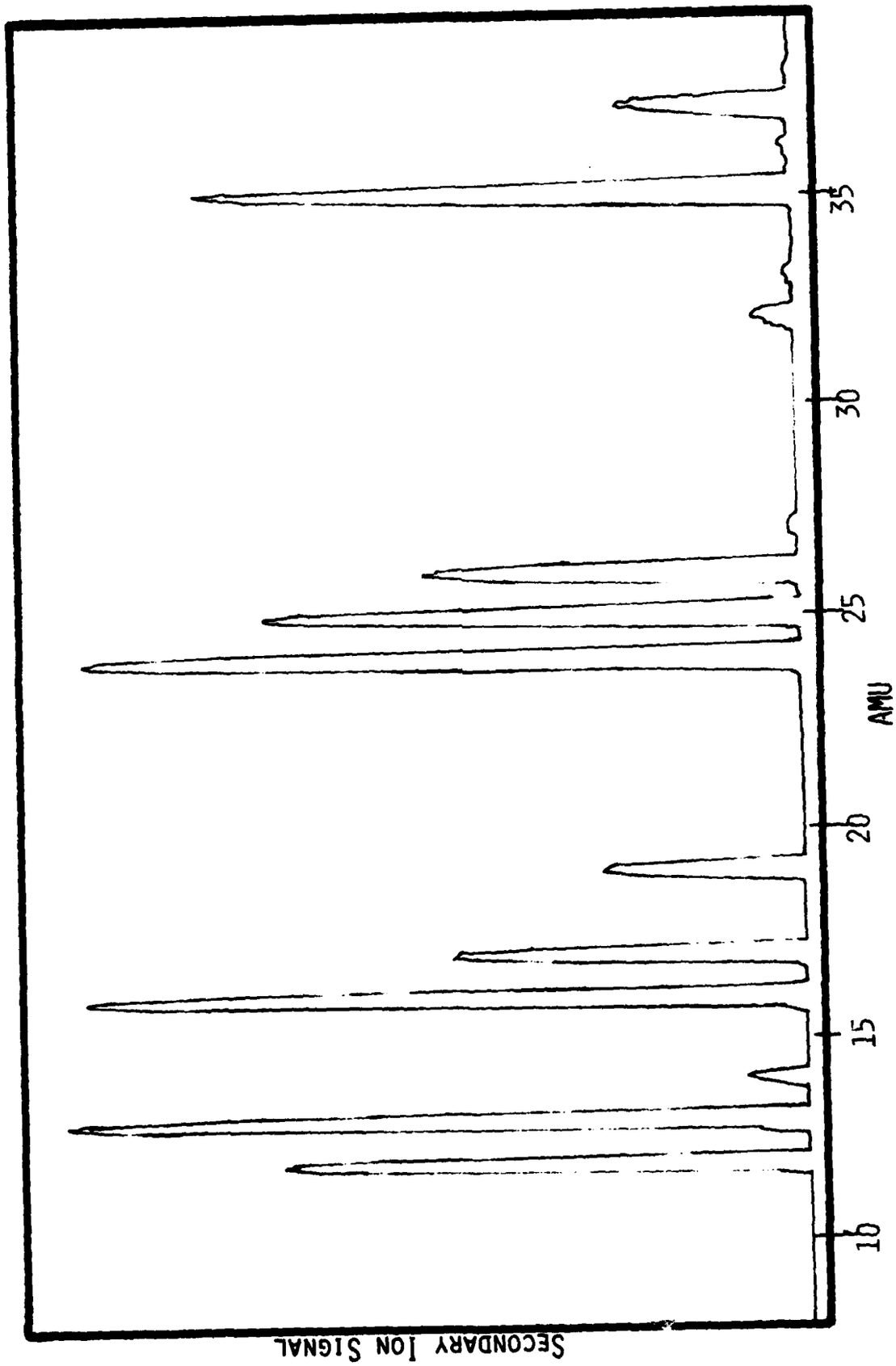

Figure 11. A Typical SIMS Spectrum for an Electron Bombarded BN Sample.

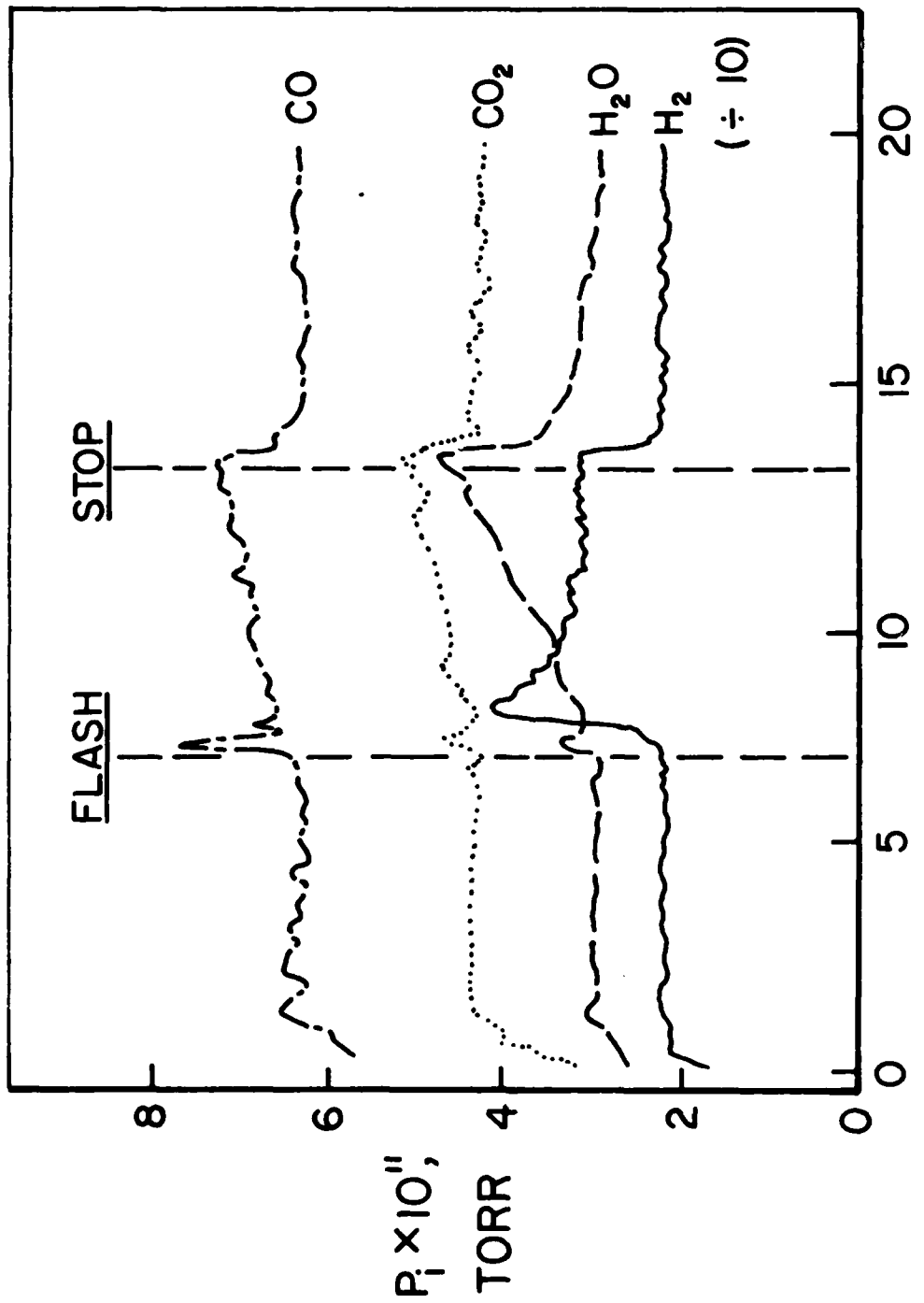

Figure 12. Typical Outgassing Curves for SAES ST-171 Non-evaporable Getter Flashed to 900°C. Approximate Partial Pressures are H_2 4×10^{-10} Torr, H_2O 5×10^{-10} Torr, CO 7×10^{-11} Torr, CO_2 4×10^{-11} Torr.

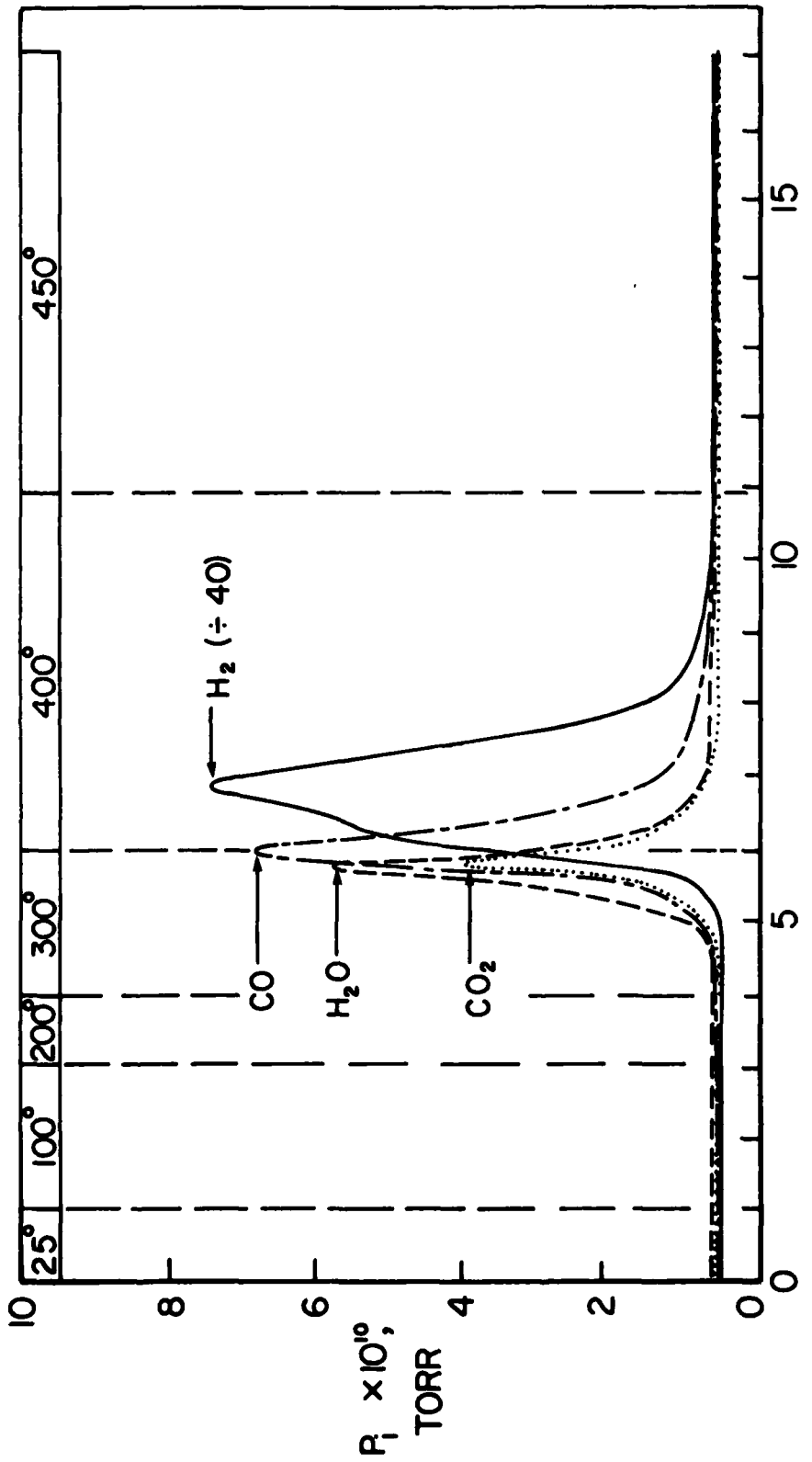

Figure 13a. Changes in Outgassing for SAES ST-171 Nonevaporable Getter Slowly Heated to 600°C.

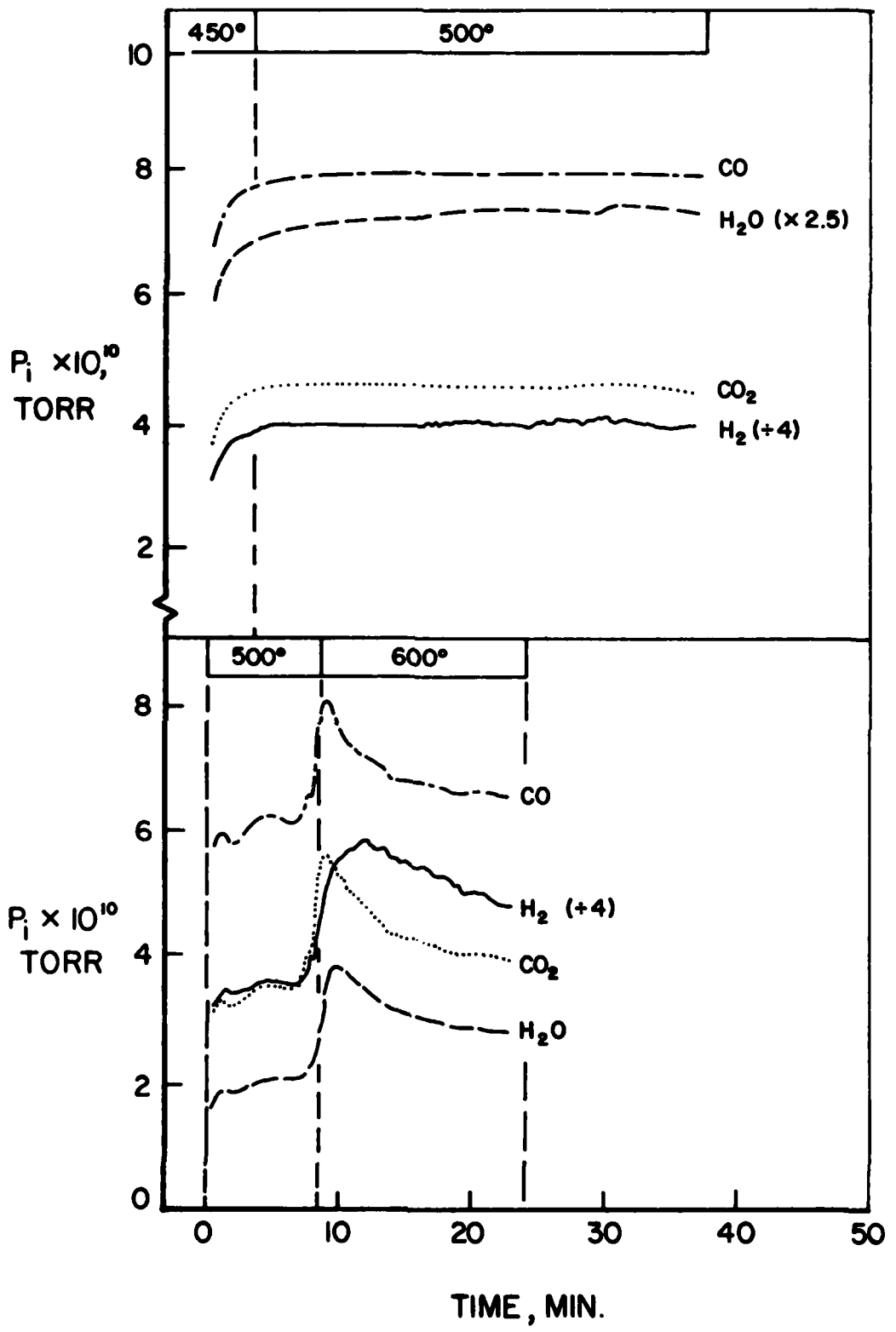

Figure 13b. Changes in Outgassing for SAES ST-171 Nonevaporable Getter Slowly Heated to 600°C.

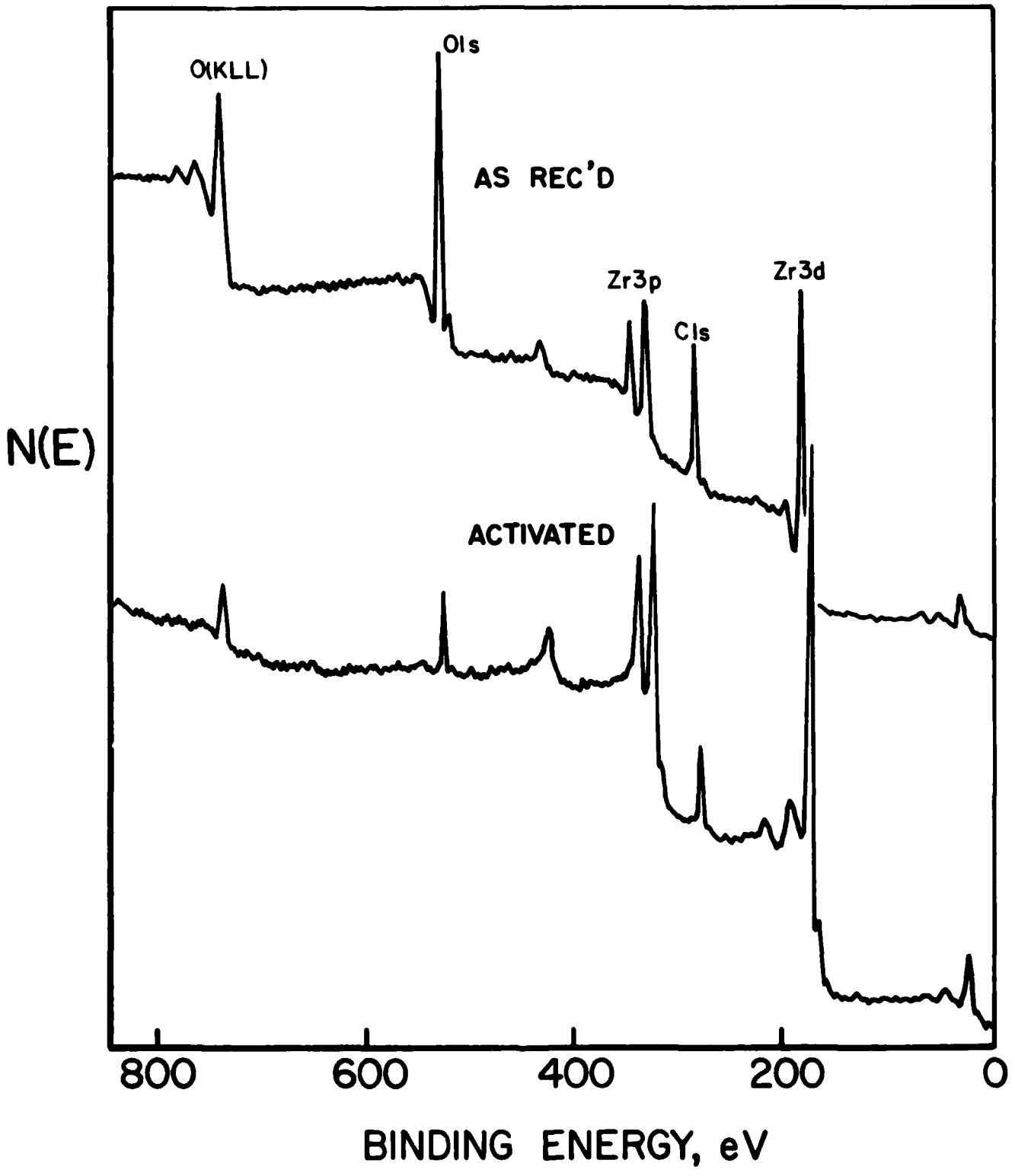

Figure 14. Photoelectron Survey Wide Scan of SAES ST-171 Non-evaporable Getter for the as Received and Activated Conditions. Referenced to Mg K_α at 1253.6eV.

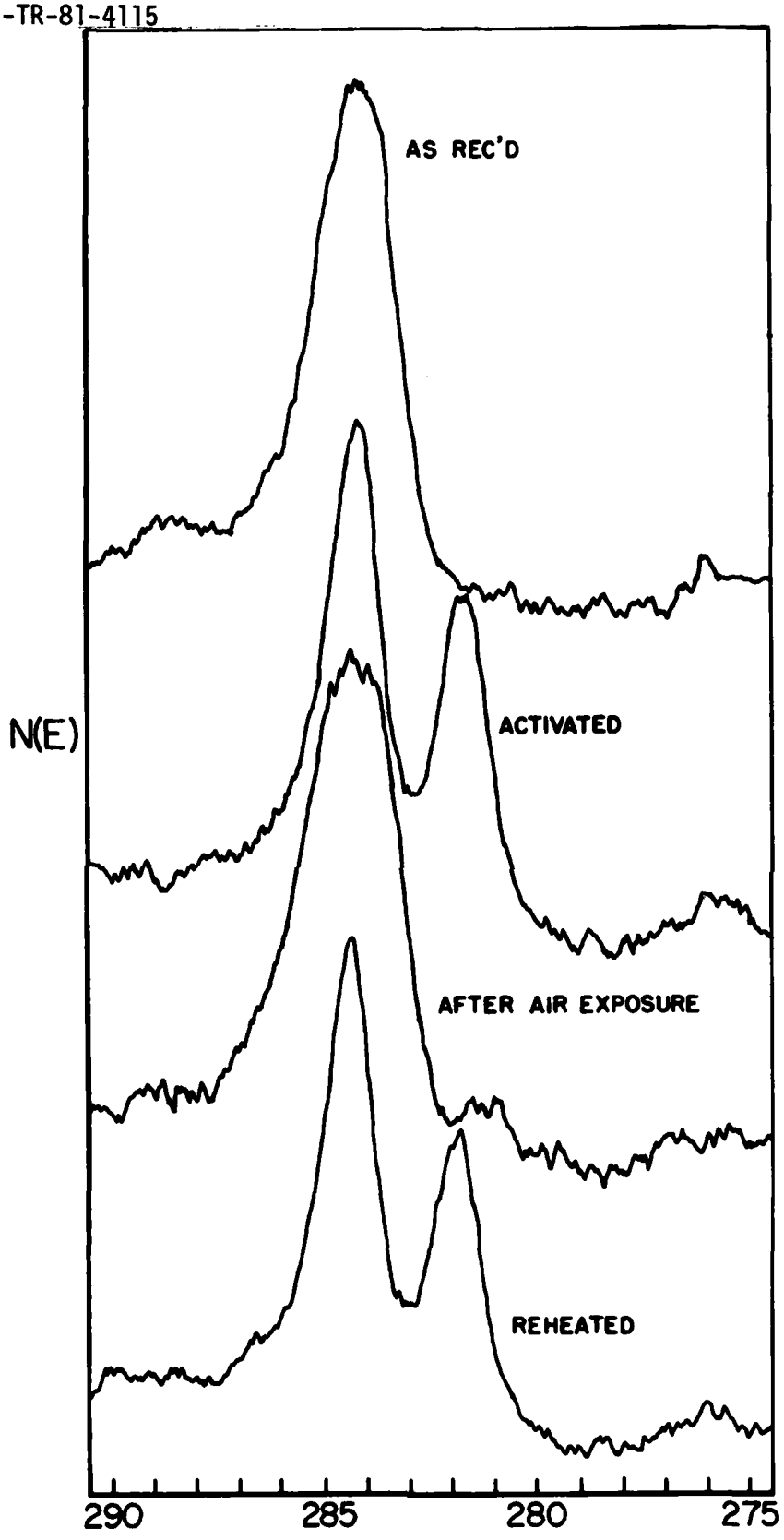

Figure 15. Photoelectrons Carbon 1s Spectra for the as Received, Activated after Air Exposure, and Reheated Conditions. Referenced to Mg K_α at 1253.6eV.

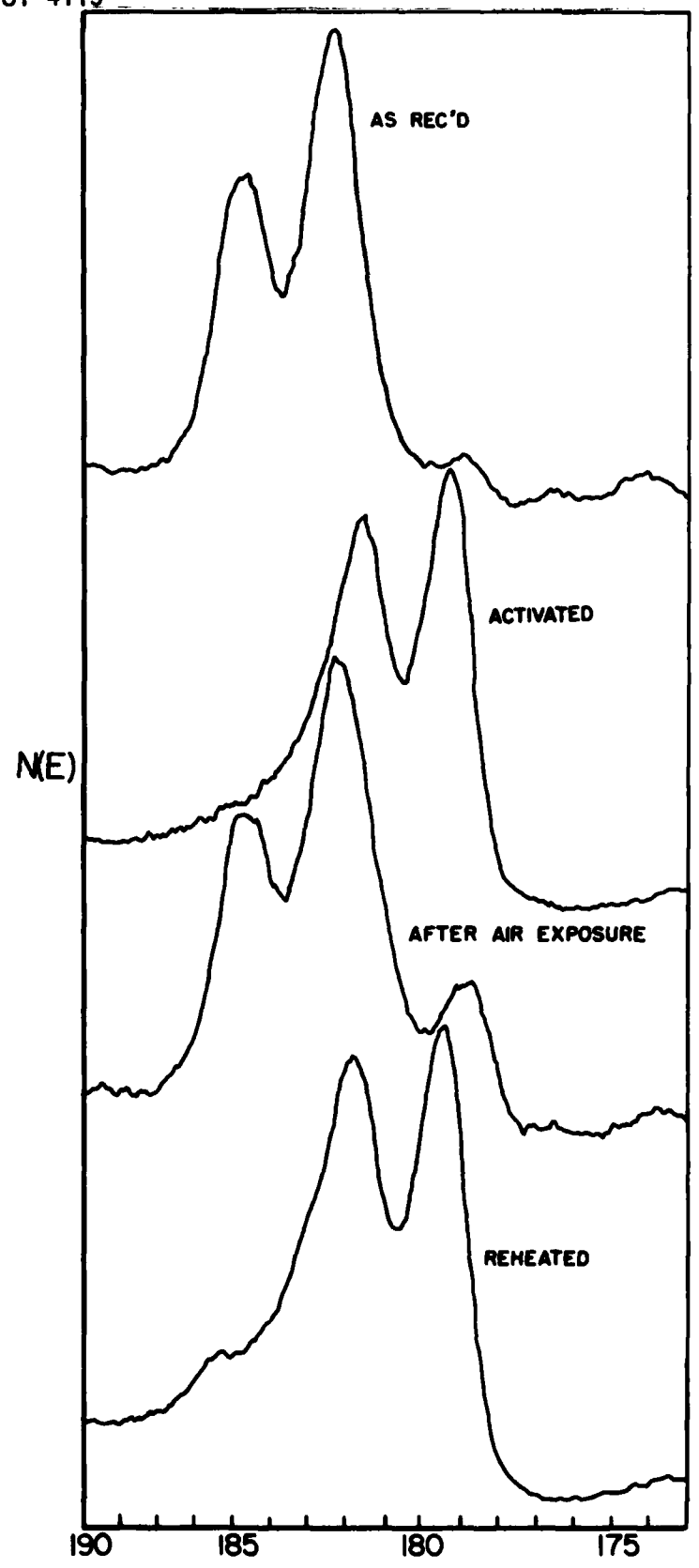

Figure 16. Zirconium 3d Photoelectron Spectra for the as Received, Activated, Air Exposed, and Reheated Conditions. Referenced to Mg K_α at 1253.6eV.

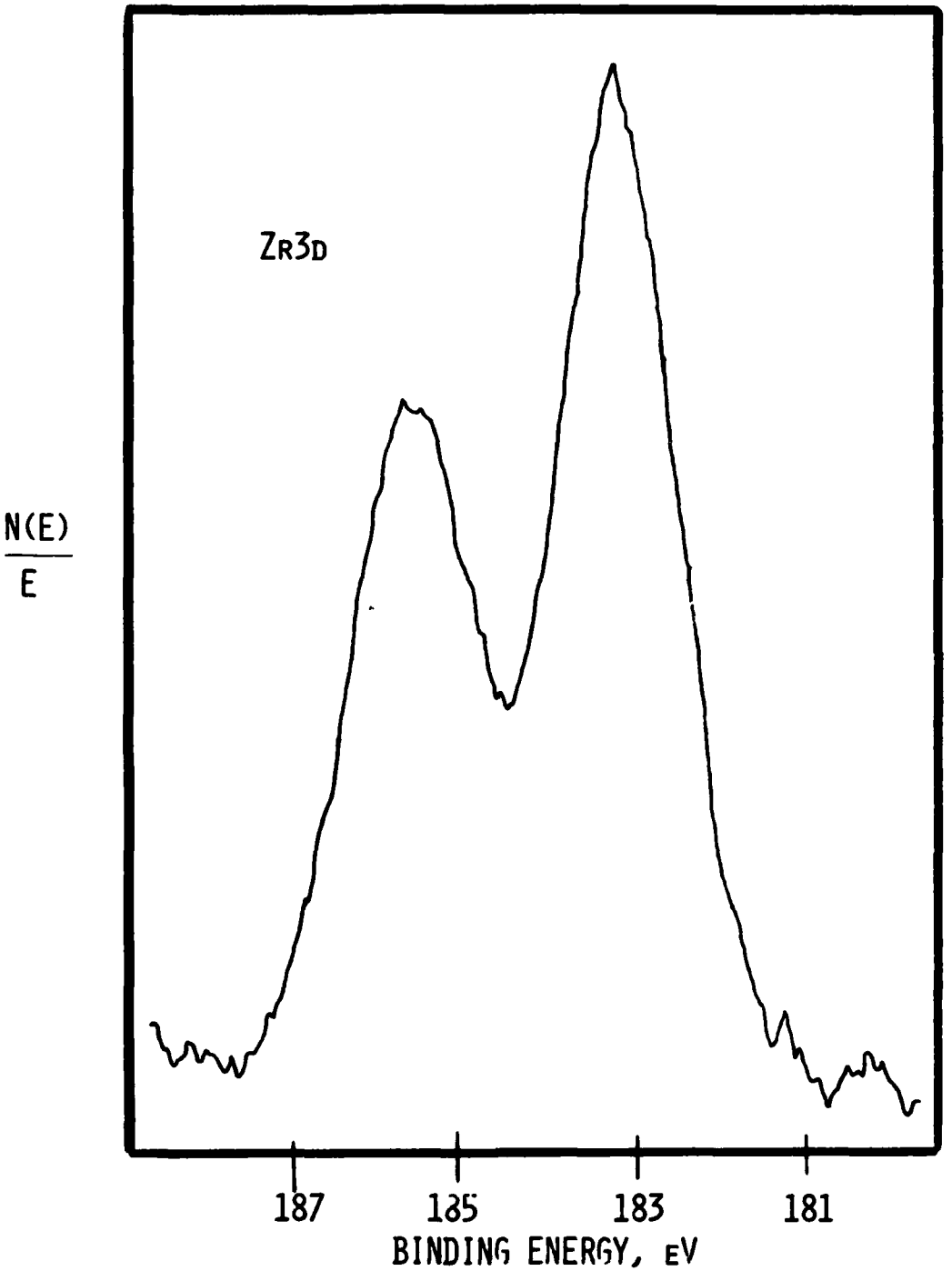

Figure 17. Zirconium 3d Photo-emission from an Ion-Bombarded Cathode Nickel Surface.

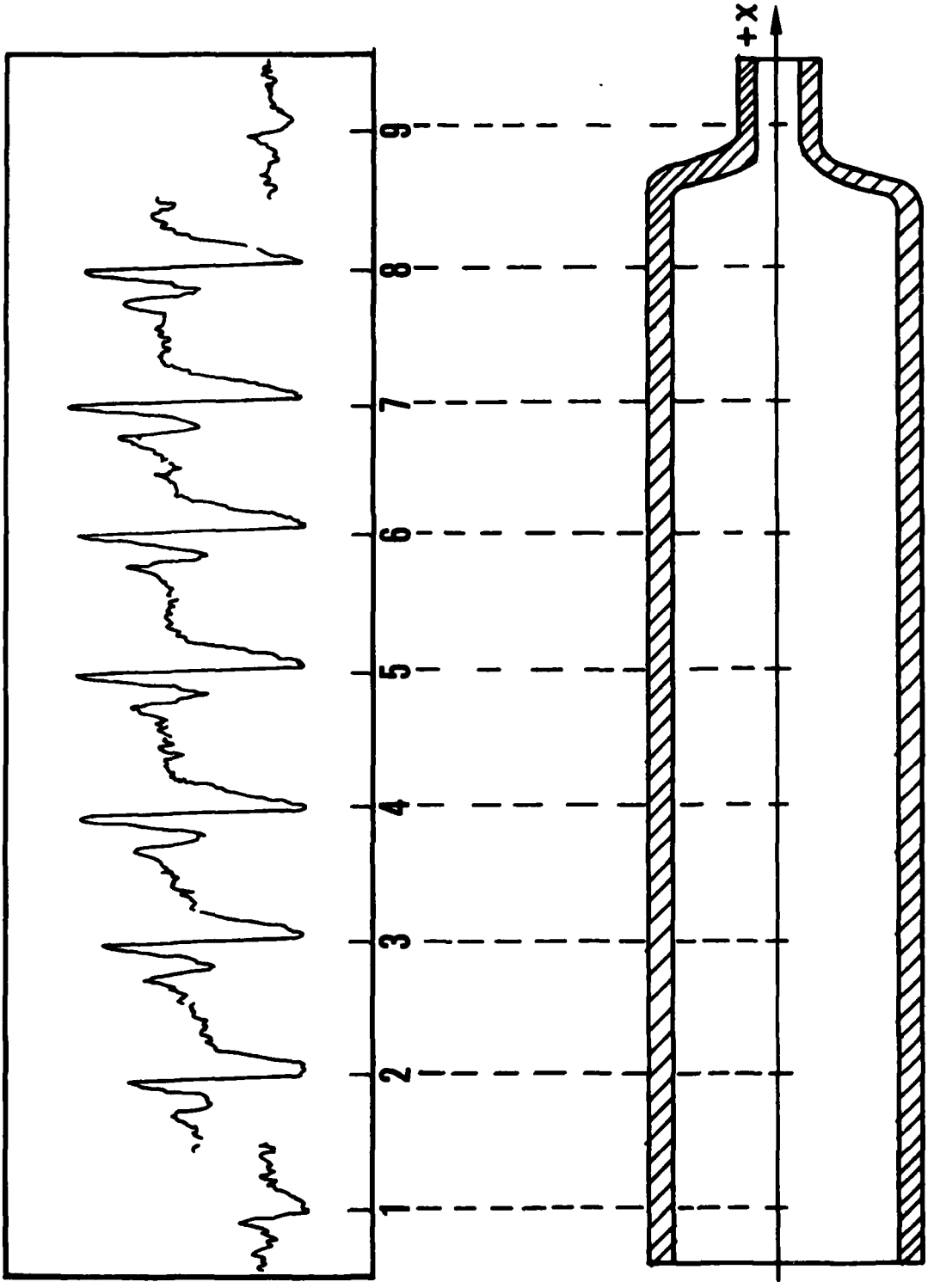

Figure 18. Nitrogen KLL Intensities as a Function of Position Along the Interior Surface of a TWT Collector.

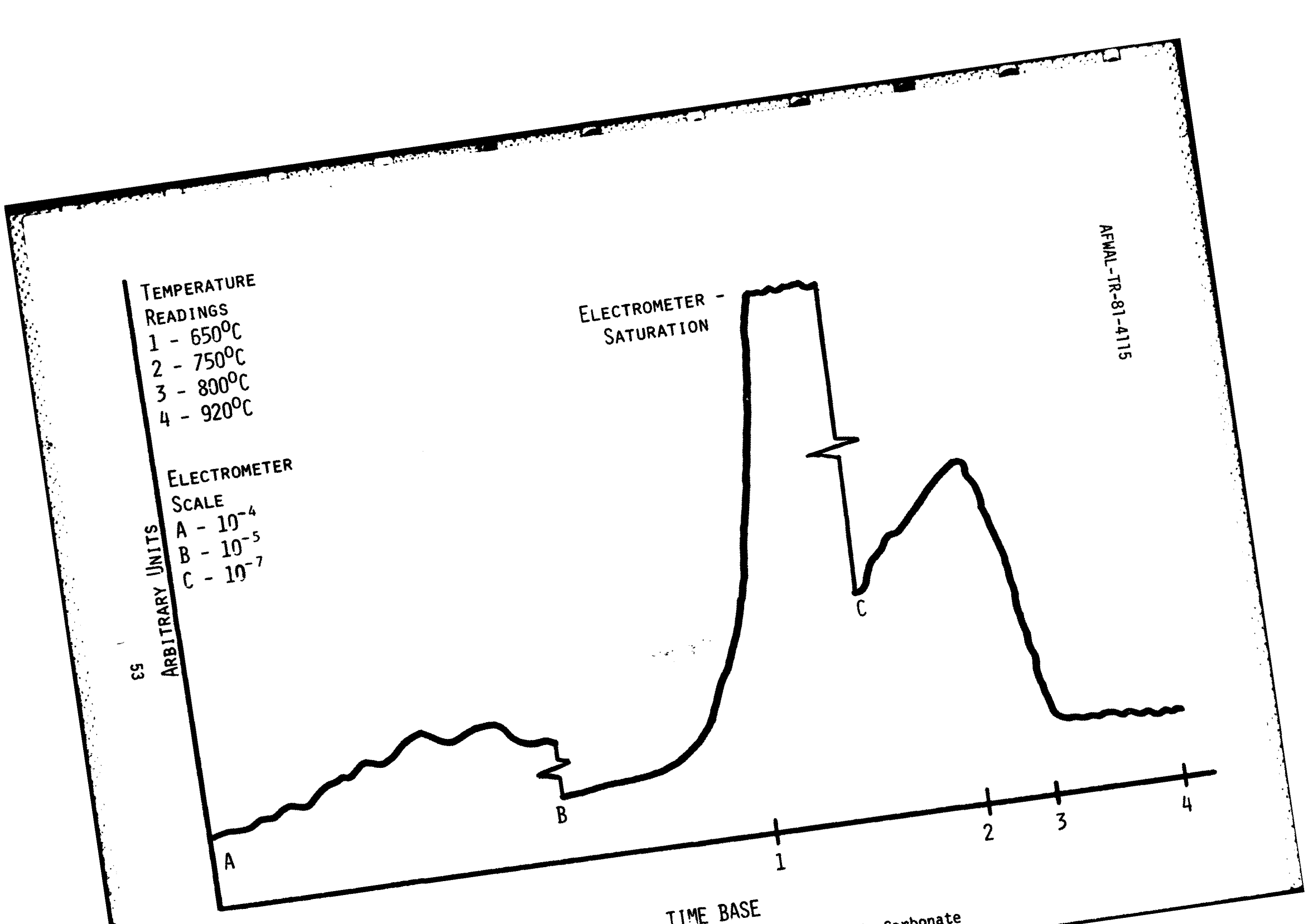

Figure 19. Evolution of CO_2 from a Typical Cathode Carbonate Material.

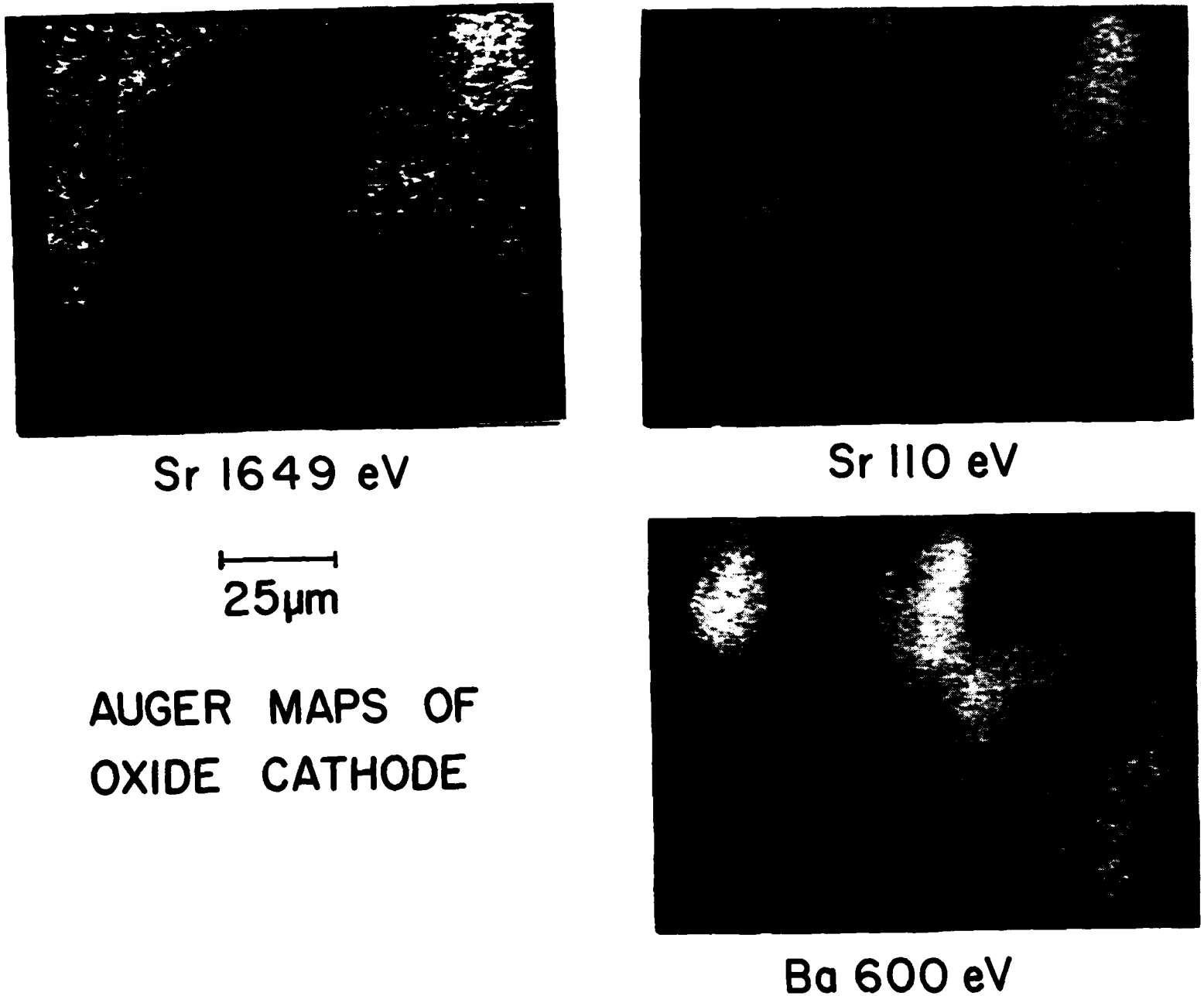

Figure 20. AES Maps of an Oxide Cathode after 50,000 Hours Operation.

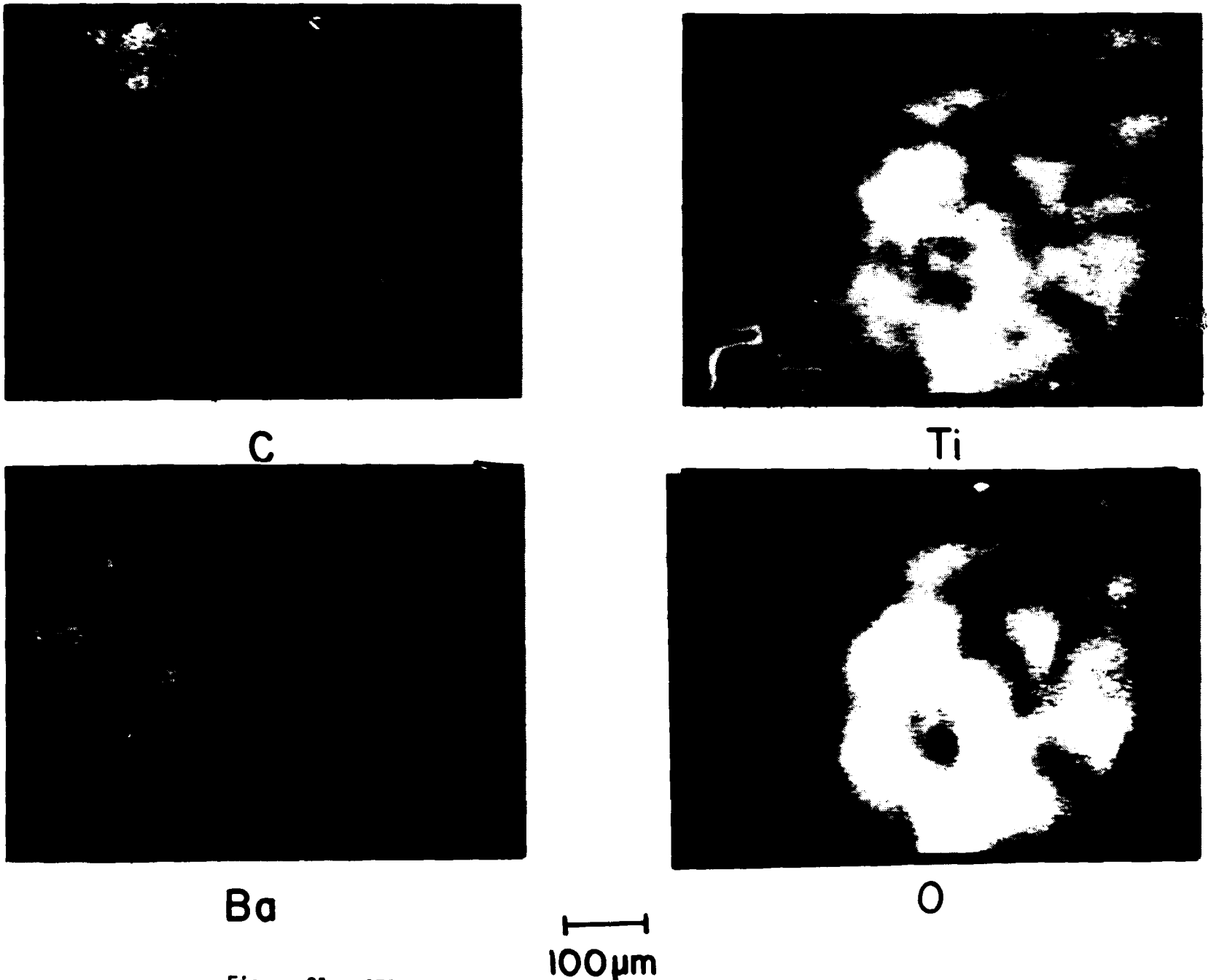

Figure 21. AES Maps of an ECM TWT Dispenser Cathode which had Low Emission Current.